# Radiative capture reactions via indirect methods

A. M. Mukhamedzhanov and G. V. Rogachev

Phys. Rev. C **96**, 045811 — Published 19 October 2017

DOI: 10.1103/PhysRevC.96.045811

# Radiative capture reactions via indirect method

A. M. Mukhamedzhanov[1*] and G. V. Rogachev[1,2†]
[1] *Cyclotron Institute, Texas A&M University, College Station, TX 77843, USA and*
[2] *Department of Physics and Astronomy, Texas A&M University, College Station, TX 77843, USA*

Many radiative capture reactions of astrophysical interest occur at such low energies that their direct measurement is hardly possible. Until now the only indirect method, which was used to determine the astrophysical factor of the astrophysical radiative capture process, was the Coulomb dissociation. In this paper we address another indirect method, which can provide information about resonant radiative capture reactions at astrophysically relevant energies. This method can be considered as an extension of the Trojan Horse method for resonant radiative capture reactions. The idea of the suggested indirect method is to use the indirect reaction $A(a, s\,\gamma)F$ to obtain information about the radiative capture reaction $A(x, \gamma)F$, where $a = (s\,x)$ and $F = (x\,A)$. The main advantage of using the indirect reactions is the absence of the penetrability factor in the channel $x + A$, which suppresses the low-energy cross sections of the $A(x, \gamma)F$ reactions and does not allow to measure these reactions at astrophysical energies. A general formalism to treat indirect resonant radiative capture reactions is developed when only a few intermediate states do contribute and statistical approach cannot be applied. The indirect method requires coincidence measurements of the triple differential cross section, which is a function of the photon scattering angle, energy and a scattering angle of the outgoing spectator-particle $s$. Angular dependence of the triple differential cross section at fixed scattering angle of the spectator $s$ is the angular $\gamma - s$ correlation function. Using indirect resonant radiative capture reactions one can obtain the information about important astrophysical resonant radiative capture reactions, like $(p, \gamma)$, $(\alpha, \gamma)$ and $(n, \gamma)$ on stable and unstable isotopes. The indirect technique makes accessible low-lying resonances, which are close to the threshold, and even subthreshold bound states located at negative energies. In this paper, after developing the general formalism, we demonstrated the application of the indirect reaction $^{12}\mathrm{C}(^{6}\mathrm{Li}, d\,\gamma)^{16}\mathrm{O}$ proceeding through $1^-$ and $2^+$ subthreshold bound states and resonances to obtain the information about the $^{12}\mathrm{C}(\alpha, \gamma)^{16}\mathrm{O}$ radiative capture at astrophysically most effective energy 0.3 MeV what is impossible using standard direct measurements. Feasibility of the suggested approach is discussed.

PACS numbers: 26.20.Fj,26.20.Np, 25.60.Tv, 25.70.Ef

## I. INTRODUCTION

Understanding the origin of the elements and stellar evolution is one of the important contemporary scientific questions in nuclear physics and astrophysics. Over 70 years ago, the concept that hydrogen and helium burning are the sources for energy production in stars was postulated in [1]. A byproduct of this burning process is the production of new elements.

It is well known today that a large number of different reactions are involved in element production. Many of these reactions take place on rather short-lived nuclei during explosive processes occurring in the cosmos. For over 50 years, experimentalists have worked to determine stellar reaction rates on systems involving stable beams and stable targets. Until recently, very little experimental information was available for reaction rates on radioactive nuclei. This is now changing with the development of new indirect techniques to determine these rates and new radioactive beam facilities that are expanding the possibilities for both direct and indirect studies. Nucleosynthesis in the Universe, i.e. the cooking processes that produce the elements of the periodic chart, proceeds through a variety of reactions and decays such as $(p,\gamma)$, $(n,\gamma)$, $(3He,\gamma)$, $(\alpha,\gamma)$, $(p,\alpha)$, $(\alpha, p)$, $(n, \alpha)$, $(\alpha, n)$, beta decays, reactions induced by gamma-quanta (photodisintegration), and neutrinos [2]. Determining the rates of these processes at stellar energies is the major part of the subject of nuclear astrophysics.

The conditions under which the majority of astrophysical reactions proceed in stellar environments make it difficult or impossible to measure them under the same conditions in the laboratory. For example, the astrophysical reactions between charged nuclei occur at energies much lower than the Coulomb barrier, which often makes the cross section of the reaction too small to measure. This is due to the very small barrier penetration factor from the Coulomb force, which produces an exponential fall off of the cross section as a function of energy. Many years ago, the astrophysical S-factor was adopted as a way to characterize cross sections by removing the Coulomb penetration factor based on an s-wave, or zero angular momentum capture. The S-factor, S(E), is defined through the relationship

$$\sigma(E) = \frac{e^{-2\,\pi\,\eta}}{S}(E). \qquad (1)$$

Here, $\sigma(E)$ is the energy-dependent cross section, $\eta$ is the

*Electronic address: akram@comp.tamu.edu
†Electronic address: rogachev@tamu.edu

Coulomb parameter of two interacting nuclei. Typically, the S-factor is the quantity that is used to extrapolate to low energies.

Indirect techniques have been developed over the past several decades to provide ways to determine reaction rates that cannot be measured in the lab. Applications of indirect methods have been undertaken with both stable and radioactive beams. There are three different commonly used indirect techniques to obtain the information about astrophysical reactions, the asymptotic normalization coefficient (ANC) approach, the Trojan Horse method (THM), and the Coulomb dissociation (CD) technique. The review of these methods is given in [3].

The ANC method in nuclear astrophysics was proposed in [4] and is based on the fact that many direct astrophysical radiative capture reactions are peripheral. Their astrophysical factor is proportional to the square of the amplitude of the overlap function. This amplitude is the ANC. The ANC method focuses on determining the normalization of the tail of the overlap function from peripheral transfer reactions whose cross sections are significantly higher than the cross sections at astrophysically relevant. Using the determined ANC one can calculate the astrophysical factor of the direct radiative capture process. Including both direct and resonant capture in a consistent framework can be done through an R-matrix analysis [5] if the relevant information is available.

The second indirect method, THM, was suggested in [6] and was modified in [7] to make it workable. It provides a powerful tool to determine the reaction rate for resonant rearrangement reactions by obtaining the cross section for a binary resonant process through the use of a surrogate Trojan Horse particle. The THM allows one to obtain the astrophysical factors of low-lying resonances which are not available by direct methods because of the absence of the penetrability factor in the entry channel of the binary sub-reaction. The theory of the THM based on the surface integral formalism [8] was presented in [3]. In [9] the combination of the ANC method and THM was applied.

The third powerful indirect technique to obtain the astrophysical factors for the radiative capture processes is the CD. The Coulomb dissociation method for nuclear astrophysics was proposed by [10] and has been tested successfully in many reactions of interest to astrophysics. The most celebrated case is the reaction $^7$Be$(p,\,\gamma)^8$B, first studied in [11], followed by numerous experiments in the last two decades [3]. The CD technique uses the virtual photon flux from the interaction of a high-energy ion with a very heavy target to dissociate the heavy ion. The dissociation is an inverse process to a capture-gamma reaction that takes place in a stellar environment. Measurements of the dissociation cross section can be used to infer the reaction rate of radiative capture processes at stellar energies. All three of these methods provide information on stellar reaction rates at very low energy without requiring an extrapolation of data from higher energies. The details of all three techniques and more references can be found in the review paper [3].

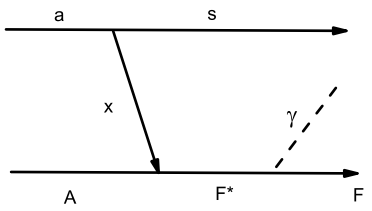


FIG. 1: Pole diagram describing the indirect radiative capture reaction proceeding through the intermediate excited state $F^*$.

In this paper, the idea of the THM is extended for the resonant radiative capture reactions. To determine the cross section for the resonant radiative capture reaction $A(x,\,\gamma)F$ we propose to use the two-step transfer reactions $A(a, s\,\gamma)F$, proceeding through the intermediate subthreshold bound states or resonances $F^* = (x\,A)^*$, with the subsequent decay of the excited state $F^* \to F + \gamma$. This approach provides a powerful indirect technique to study radiative capture processes $A(s,\,\gamma)F$ and, in particular, the astrophysical radiative capture reactions. The mechanism of such processes is shown in Fig. 1, where $a = (s\,x)$ and $F = (x\,A)$ are the ground bound states of $a$ and $F$. Note that diagram in Fig. 1 can be obtained from the similar diagram in the THM (see Fig. 2 [3]) by replacing the particle's line $b$ by the photon's line $\gamma$.

Such indirect reactions allow one to invade into the region previously unthinkable if we would rely only on direct measurements. Among of the important reactions, which require a broader approach than only direct measurements, are low-energy astrophysical radiative capture processes, such as $(p,\,\gamma)$, $(\alpha,\,\gamma)$ and $(n,\,\gamma)$ [2] on stable and unstable isotopes performed in direct and inverse kinematics. Among these reactions, without any doubt, is the most important one, the so-called, "holy grail" reaction $^{12}\mathrm{C} + \alpha \to {}^{16}\mathrm{O}(0^+, E_x = 0.0\mathrm{MeV}) + \gamma$, which dominates the helium burning in red giants [2]. The indirect reactions provide a perfect tool to study radiative capture reactions at astrophysically relevant energies.

We present the theory of the indirect method to treat the resonant radiative capture processes when only a few subthreshold bound states and resonances are involved, and statistical methods cannot be applied. The developed formalism is based on the generalized multi-level $R$-matrix approach and surface integral formulation of the transfer reactions, which are the first stage of the indirect reaction mechanism described by the diagram in Fig. 1 [3]. By the generalized $R$-matrix approach we mean the $R$ -matrix method applied for $2 \to 3$ particle

reactions rather than to binary $2 \to 2$ particle reactions. We also describe the methodology of the indirect radiative capture experiment. There are many papers devoted to the angular correlation of the photons emitted in nuclear transfer reactions with final nuclei, see, for example, [12] and references therein. Here we apply the generalized $R$-matrix to develop the formalism allowing one to study the photon's angular distribution correlated with the scattering angle of one of the final nuclei formed in the transfer reaction.

Developing quite a general formalism we keep in mind, in particular, the application of the method for the $^{12}$C($^6$Li, $d\,\gamma$)$^{16}$O reaction, which can provide important information about the astrophysical $^{12}$C($\alpha$, $\gamma$)$^{16}$O process. This astrophysical reaction is contributed by two interfering subthreshold resonances ([2], sect. 4.5). We note that a bound state, which is close to the threshold, is also called a subthreshold resonance. The elastic scattering cross section in the presence of subthreshold bound states has a peak at zero energy, that is, it behaves like a resonance cross section with a resonance close to the threshold. Also, the subthreshold bound state may reveal itself as a resonance in the case of the radiative capture, which can occur to the wing of the subthreshold state at positive energy forming the intermediate excited state.

Subthreshold resonances play an important role in many astrophysical processes. Often, using direct measurements, it is quite difficult or impossible to reach the astrophysically relevant energy region where the subthreshold resonances manifest themselves. However, the region, where the contribution of the subthreshold resonances is important, can be reached using indirect reactions [3, 13]. For more details regarding subthreshold resonances and how they are handled in the $R$-matrix approach see [13]. The excited bound state subsequently decays to lower lying states by emitting a photon. In this case, the subthreshold bound state is characterized by a resonance width in complete analogy with the real resonance [51]. Besides the subthreshold resonances, we also take into account the real resonances located at positive energies.

Numerous attempts to obtain the astrophysical factor of the $^{12}$C($\alpha$, $\gamma$)$^{16}$O reaction, both experimental and theoretical, have been made for almost 50 years [14–50]. This reaction is contributed by interfering $E1$ and $E2$ transitions. The $E1$ transition is complicated by the interference of the capture through the wing of the subthreshold $1^-$ resonance at $-0.045$ MeV with the low-energy tail of the resonance $1^-$, $E_{\alpha\,^{12}\mathrm{C}} = 2.423$ MeV, where $E_{\alpha\,^{12}\mathrm{C}}$ is the $\alpha - {}^{12}$C relative kinetic energy. The $E2$ transition is dominated by the capture to the ground state of $^{16}$O through the wing of the subthreshold bound state $2^+$, $E_{\alpha\,^{12}\mathrm{C}} = -0.245$ MeV. In addition, to fit the experimental data, usually a few artificial levels are added to fit $E1$ and $E2$ data [24, 27]. The difficulty of the direct measurements of the $E1$ transition can be easily understood if even in the peak of the resonance at $1^-$, $E_{\alpha\,^{12}\mathrm{C}} = 2.423$ MeV the cross section is only about $40 - 50$ nb [44–46] . Moreover , the $E1$ transition from $1^-$ states to the ground state of $^{16}$O is isospin forbidden for $T = 0$ components and is possible only due to the small admixture of the $T = 1$ components.

Extremely small penetrability factor at $E_{\alpha\,^{12}\mathrm{C}} \leq 1$ MeV makes it impossible or very difficult to measure the astrophysical factor for the $^{12}$C($\alpha$, $\gamma$)$^{16}$O reaction at energies $E_{\alpha\,^{12}\mathrm{C}} \leq 1$ MeV with reasonable accuracy. For the sensitivity of the extracted astrophysical factor from the existing data, see works [37, 39, 41]. Note that from the astrophysical point of view the required uncertainty of this astrophysical factor at $E_{\alpha\,^{12}\mathrm{C}} \sim 0.3$ MeV should be $\leq 10\%$. New gamma-ray facilities, an upgraded gamma-source (HIGS2) [47] in USA and Compton gamma-ray source of Eli-NP [48] in Romania, are supposed to measure the astrophysical factor for the $^{12}$C($\alpha$, $\gamma$)$^{16}$O reaction down to 1 MeV.

In this paper we discuss a completely new method of measuring the astrophysical factor $S(E_{\alpha\,^{12}\mathrm{C}})$ for the $^{12}$C($\alpha$, $\gamma$)$^{16}$O reaction down to astrophysical energies $\sim 300$ keV. This method is based on the coincidence measurements of the deuterons and the photons from the indirect reaction $^{12}$C($^6$Li, $d\,\gamma$)$^{16}$O. In the indirect method the absolute value of the triple differential cross section is determined by its normalization to the available direct data at higher energies.

The suggested technique allows one not only to determine the astrophysical $S$ factor down to energies $E_{\alpha\,^{12}\mathrm{C}} \sim 0.3$ MeV but also the interference pattern between the subthreshold bound state and higher resonance for the $E1$ transition. We use the surface-integral formalism [8] in which the matrix elements are expressed in terms of the external radial overlap functions and do not depend on the $R$-matrix hard-sphere scattering phase shifts. Hence, when considering the interference of the $E1$ and $E2$ matrix elements, the $R$-matrix hard-sphere phase shifts do not appear. The method, which we address here, can be used for a broader type of radiative capture experiments $A(a,\, s\,\gamma)F$ proceeding through the subthreshold and real resonances.

## II. THEORY

We follow the THM idea and extend it for the radiative capture reaction. To measure the cross section of the binary process

$$x + A \to F^* \to \gamma + F \tag{2}$$

proceeding through the intermediate resonance $F^*$ at astrophysical energies we suggest to measure the surrogate reaction (two-body to three-body process ($2 \to 3$ particles)):

$$a + A \to s + F^* \to s + \gamma + F \tag{3}$$

in the vicinity of the quasi-free (QF) kinematics [3]. Here the incident particle, $a = (s\,x)$, which has a dominant

cluster structure, is accelerated at energies above the Coulomb barrier. The reaction (3) is a two-stage process. On the first stage the transfer reaction $a + A \to s + F^*$ populating the wing of the subthreshold bound state at $E_{xA} > 0$ or the real resonance occurs. On the second stage, the excited state $F^*$ decays to the ground state $F$ by emitting a photon. From the measured energy dependence of the cross section of the reaction (3), the energy dependence of the binary sub-process (2) is determined. By normalizing the measured cross section to the available direct one(s) measured at higher energies with better accuracy one can get the absolute value of the astrophysical $S$ factor at low energies.

The mechanism of the indirect reaction shown schematically in Fig. (1) gives the dominant contribution to the cross section in a restricted region of the three-body phase space when the relative momentum of the fragments $s$ and $x$ is zero (the quasi-free (QF) kinematical condition) or less than the wave number of the bound state $a = (s\,x)$. Since the transferred particle $x$ is virtual, its energy and momentum are not related by the on-shell equation, that is, $E_x \neq k_x^2/(2\,m_x)$.

The main advantage of the indirect method is that the penetrability factor in the entry channel of the binary reaction (2) is not present in the expression for the indirect reaction cross section. It allows one to measure the resonant reaction (2) cross section at astrophysically relevant energies at which direct measurements are impossible or extremely difficult because of the presence of the penetrability factor in the binary reaction cross section. Moreover, the indirect method allows one to measure the cross section of the binary reaction (2) even at negative $E_{xA}$ owing to the off-shell character of the transferred particle $x$ in reaction (3).

The expression for the amplitude of the transfer reaction (3) ( for $x = n$) in the surface integral approach and distorted wave Born approximation (DWBA) was derived in [8]. It is assumed, similar to the THM [3], that only the energy dependence of the cross section of the reaction (3) is measured, while its absolute value is determined by normalizing the cross section of the reaction (3) to the available direct experimental data at higher energies. That is why it makes sense to use the plane wave approximation to get the indirect reaction amplitude. The comparison of the plane wave impulse approximation (PWIA) and DWBA has been done in many THM papers [3, 9, 52–54]. In these papers, the momentum distribution of the spectator was calculated in plane wave and DWBA. Both calculations agreed with each other and experimental data within the range of the QF peak. The most detailed comparison of the PWIA and DWBA was done in [54]. It was confirmed again that the angular distribution of the spectator calculated in the DWBA and PWIA agree quite well within the QF peak. A further probe of the reliability of the plane-wave approach in describing the experimental data came from the comparison between plane-wave-Born approximation (PWBA) and DWBA calculations. The differences in the ratios of the integrated resonance cross sections calculated in plane-wave and DWBA approaches are less than 19%, compared with the experimental uncertainties. Therefore, when no absolute values of the cross sections are extracted, the PWIA description is more preferable than DWBA because PWBA does not depend on the optical potentials which are not known accurately at low energies.

In this paper, we, for the first time, present the general equations of the indirect reaction triple differential and double cross sections to be used for the analysis of the radiative reactions proceeding through the subthreshold and isolated resonances. The system of units in which $\hbar = c = 1$ is being used throughout of the paper.

### A. Indirect reaction amplitude for the resonant radiative capture

Let us consider the radiative capture reaction (2) proceeding through the wing (at $E_{xA} > 0$) of the subthreshold bound state (aka subthreshold resonance) $F^* = F^{(s)}$, where $F^{(s)} = (x\,A)^{(s)}$ or real resonance at $E_{xA} > 0$. We assume that both can decay to the ground state $F = (xA)$. To measure the cross section of this reaction at astrophysically relevant energies where subthreshold resonances can be important, for the reasons explained above, we use the indirect reaction (3). First, we derive the reaction amplitude of the indirect radiative capture process and then the triple differential cross section of reaction (3). After that, by integrating over the angles of the emitted photons, we get the double differential cross section. The interference of the subthreshold bound state and the resonance, which both decay to the ground state $F = (xA)$, is taken into account. Evidently that this case can be applied for the $E1$ and $E2$ transitions of the reaction $^{12}\mathrm{C}(\alpha,\gamma)^{16}\mathrm{O}$.

To describe the radiative capture to the ground state through two interfering states we use the single channel, two-level generalized $R$-matrix equations developed for the three-body reactions 2 *particles* $\to$ 3 *particles* [3, 8]. We also take into account the interference of transitions with different multipolarities $L$. Thus, we take into account the interference of radiative decays from different levels with the same multipolarity and interference of transitions from various levels with different multipolarities.

The indirect reaction described by the diagram of Fig. (1) proceeds as a two stage process. The first part is transfer of particle $x$ (stripping process) to the excited state $F_\tau$, $\tau = 1, 2$, where $F_1 = F^{(s)}$ is the subthreshold resonance and $F_2$ is the resonance state at $E_{xA} > 0$. No gamma is emitted during the first stage. On the second stage the excited state $F_\tau$ decays to the ground state $F = (xA)$ by emitting a photon. Then the indirect reaction amplitude followed by the photon emission from the intermediate subtheshold resonance and resonance takes

the form:

$$M^{M_s\,M\,M_F}_{M_a\,M_A} = \sum_{\tau,\nu=1}^{2} \sum_{M_{F^{(s)}_\nu}\,M_{F^{(s)}_\tau}} V^{M_F\,M}_{M_{F^{(s)}_\nu}\,\nu}\,\mathbf{A}_{\nu\,\tau}\,M^{M_s\,M_{F^{(s)}_\tau}}_{M_a\,M_A\,\tau}\,. \tag{4}$$

Here $M_i$ is the projection of the spin $J_i$ of the particle $i$, $M_{F^{(s)}_\tau}$ is the projection of the spin $J_{F^{(s)}}$ of the subthreshold resonance ($\tau = 1$) and resonance ($\tau = 2$), $M$ is the projection of the angular momentum of the emitted photon. Also 2 is the number of the level included. We assume that the spins of the subthreshold resonance and real resonance are equal $F_1 = F_2 = F^{(s)}$ and these resonances do interfere. At the moment we confine ourselves by transition with one multipolarity $L$. That is why the index $L$ is omitted. Later on we take into account transitions with different $L$. $M^{M_s\,M_{F^{(s)}_\tau}}_{M_a\,M_A\,\tau}$ is the amplitude of the direct transfer reaction

$$a + A \to s + F_\tau \tag{5}$$

populating the intermediate excited state $F_\tau$. The reaction (5) is the first stage of the indirect reaction (3). $V_\nu$ is the amplitude of the radiative decay of the excited state $F_\nu$ ($\nu = 1, 2$) to the ground state $F = (xA)$, $\mathbf{A}_{\lambda\,\tau}$ is the matrix element of the level matrix in the $R$-matrix method.

In the prior form of the plane-wave approximation $M^{M_s\,M_{F^{(s)}_\tau}}_{M_a\,M_A\,\tau}$ takes the form:

$$M^{M_s\,M_{F^{(s)}_\tau}}_{M_a\,M_A\,\tau}(\mathbf{k}_{sF_\tau}, \mathbf{k}_{aA}) = < \chi^{(0)}_{\mathbf{k}_{sF_\tau}}\,\Phi_\tau\,\big|V_{xA}\big|\varphi_{sx}\,\varphi_A\,\chi^{(0)}_{\mathbf{k}_{aA}} > . \tag{6}$$

Here, $\Phi_1$ is the bound-state wave function of the subthreshold bound state $F_1 = (xA)^{(s)}$, $\Phi_2$ is the $F_2$ resonance wave function, $\varphi_{sx}$ and $\varphi_A$ are the bound-state wave functions of $a = (s\,x)$ and $A$, respectively, $\chi^{(0)}_{\mathbf{k}_{aA}} = e^{i\,\mathbf{k}_{aA}\cdot\mathbf{r}_{aA}}$ and $\chi^{(0)}_{\mathbf{k}_{sF_\tau}} = e^{i\,\mathbf{k}_{sF_\tau}\cdot\mathbf{r}_{sF}}$ are the planes waves in the initial and final states of the reaction (5), respectively, $\mathbf{r}_{ij}$ is the radius-vector connecting the centers of mass of nuclei $i$ and $j$, $\mathbf{k}_{aA}$ is the $a - A$ relative momentum in the initial state of the reaction (5) and $\mathbf{k}_{sF_\tau}$ is the $s - F_\tau$ relative momentum in the final state of this transfer reaction, $V_{xA}$ is the $x - A$ interaction potential.

In the matrix element $M^{M_s\,M_{F^{(s)}_\tau}}_{M_a\,M_A\,\tau}(\mathbf{k}_{sF_\tau}, \mathbf{k}_{aA})$ we introduce in the bra state the projection operator $\sum\limits_n |\varphi_{A_n} >< \varphi_{A_n}|$, where the sum over $n$ is taken over the bound and continuum states of nucleus $A$. In the projection operator we keep only the projection on the ground state of $A$. Then Eq. (6) can be rewritten as

$$M^{M_s\,M_{F^{(s)}_\tau}}_{M_a\,M_A\,\tau}(\mathbf{k}_{sF_\tau}, \mathbf{k}_{aA}) = < \chi^{(0)}_{\mathbf{k}_{sF_\tau}}\,\Upsilon_\tau\,\big|\overline{V}_{xA}\big|\varphi_{sx}\,\chi^{(0)}_{\mathbf{k}_{aA}} >, \tag{7}$$

where $\overline{V}_{xA} = < \varphi_A|V_{xA}|\varphi_A >$. Also,

$$\Upsilon_\tau(\mathbf{r}_{xA}) = < \varphi_A\,\big|\Phi_\tau > = \sum_{m_{j_i}\,m_{l_i}} < j_i\,m_{j_i}\;l_i\,m_{l_i}\big|J_{F^{(s)}}\,M^{(s)}_{F_\tau} > \times < J_x\,M_x\;J_A\,M_A\big|j_i\,m_{j_i} > \Upsilon_{\tau\,j_i\,l_i\,J_{F^{(s)}}}(r_{xA})\,Y_{l_i\,m_{l_i}}(\hat{\mathbf{r}}_{xA}) \tag{8}$$

is the projection of the wave function $\Phi_\tau$ on the ground state wave function of $A$, $\Upsilon_{\tau\,j_i\,l_i\,J_{F^{(s)}}}(r_{xA})$ is its radial part, $j_i\,(m_{j_i})$ is the channel spin (its projection) of $x + A$ and $l_i\,(m_{l_i})$ is their orbital angular momentum (its projection) at which the subthreshold resonance and resonance occur in the channel $x + A$, $< j_i\,m_{j_i}\;l_i\,m_{l_i}\big|J_{F^{(s)}}\,M^{(s)}_{F_\tau} >$ is the Clebsch-Gordan coefficient, $Y_{l_i\,m_{l_i}}(\hat{\mathbf{r}}_{xA})$ is the spherical harmonic, $\hat{\mathbf{r}} = \mathbf{r}/r$.

$\Upsilon_{\tau\,j_i\,l_i\,J_{F^{(s)}}}(r_{xA})$ is the radial part of $\Upsilon_\tau(\mathbf{r}_{xA})$ in the state $\tau$ with the channel spin $j_i$ and the orbital angular momentum $l_i$. Since we assume that both levels $\tau = 1$ and $\tau = 2$ do interfere, $j_i$ and $l_i$ are the same for both levels. We assume that only one $j_i$ and $l_i$ contribute to the reaction. It is important to underscore that, although the subthreshold resonance is located at $E_{xA} = -\varepsilon^{(s)}_{xA}$, the capture occurs to its wing at $E_{xA} > 0$. Hence, $\Upsilon_{1\,j_i\,l_i\,J_{F^{(s)}}}(r_{xA})$ is described by the resonance radial wave function, which we take in the $R$-matrix form. We also take the radial overlap $\Upsilon_{2\,j_i\,l_i\,J_{F^{(s)}}}(r_{xA})$ in the form of the $R$-matrix resonant wave function. It has been shown in [3] that in the surface integral approach the dominant contribution to the prior form of the transfer reaction amplitude comes from the external region $r_{xA} \geq R_{xA}$. In the external region we take the resonance wave function as [8]

$$\Upsilon_{\tau\;j_i\,l_i\,J_{F^{(s)}}}(r_{xA}) = \sqrt{\frac{\mu_{xA}}{k_{xA}}\,\Gamma_{\tau\,j_i l_i J_{F^{(s)}}}}\;e^{-i\,\delta^{hs}_{l_i}}\;\frac{O_{l_i}(r_{xA})}{r_{xA}}, \tag{9}$$

where

$$O_{l_i}(r_{xA}) = i\,F_{l_i}(k_{xA},\,r_{xA}) + G_{l_i}(k_{xA},\,r_{xA}) = e^{\,i\,\delta^{hs}_{l_i}}\,\sqrt{F^2_{l_i}(k_{xA},\,r_{xA}) + G^2_{l_i}(k_{xA},\,r_{xA})} \tag{10}$$

is the outgoing spherical wave in the partial wave $l_i$, $F_{l_i}$ and $G_{l_i}$ are the Coulomb regular and singular solutions, $\delta^{hs}_{l_i}$ is the $R$-matrix hard-sphere scattering phase shift. From Eqs. (9) and (10) is clear that $\Upsilon_{\tau\;j_i\,l_i\,J_{F^{(s)}}}(r_{xA})$ does not depend on the $R$-matrix hard-sphere scattering phase shift.

At $r_{xA} = R_{xA}$ we get

$$\Upsilon_{\tau\;j_i\,l_i\,J_{F^{(s)}}}(R_{xA}) = \sqrt{\frac{2\,\mu_{xA}}{R_{xA}}}\,\gamma_{\tau\,j_i l_i J_{F^{(s)}}}. \tag{11}$$

We see that $\Upsilon_{\tau\;j_i\,l_i\,J_{F^{(s)}}}(R_{xA})$ does not depend on $\delta^{hs}_{l_i}$.

$\Gamma_{\tau\,j_i l_i J_{F^{(s)}}}$ is the formal resonance width in the $R$-matrix approach for the level $\tau$, which is related to the reduced width amplitude $\gamma_{\tau\,j_i l_i J_{F^{(s)}}}$ of the level $\tau$ as [55]

$$\Gamma_{\tau\,j_i l_i J_{F^{(s)}}} = 2\,P_{l_i}(E_{xA},\,R_{xA})\,\gamma^2_{\tau\,j_i l_i J_{F^{(s)}}}. \tag{12}$$

Here, $P_{l_i}(E_{xA},\,R_{xA})$ is the barrier penetrability factor, $R_{xA}$ is the channel radius, Equation (12) holds at $E_{xA} > 0$ both for the subthreshold resonance and resonance.

The observable resonance width is expressed in terms of the observable reduced width by [55]

$$\tilde{\Gamma}_{\tau\,j_i l_i J_{F^{(s)}}} = 2\,P_{l_i}(E_{xA},\,R_{xA})\,\tilde{\gamma}^2_{\tau\,j_i l_i J_{F^{(s)}}}, \tag{13}$$

where the observable and formal reduced widths $\tilde{\gamma}^2_{\tau\,j_i l_i J_{F^{(s)}}}$ and $\gamma^2_{\tau\,j_i l_i J_{F^{(s)}}}$, respectively, are related by [55]

$$\tilde{\gamma}^2_{\tau\,j_i l_i J_{F^{(s)}}} = \frac{\gamma^2_{\tau\,j_i l_i J_{F^{(s)}}}}{1 + \gamma^2_{\tau\,j_i l_i J_{F^{(s)}}}\,[\mathrm{d}S_{l_i}(E_{xA})/\mathrm{d}E_{xA}]\big|_{E_{xA}=E_\tau}}. \tag{14}$$

$E_1 = -\varepsilon^{(s)}_{xA}$ and $E_2 = E_R$, where $E_R$ is the resonance energy corresponding to the level $\tau = 2$. The inverse equation is

$$\gamma^2_{\tau\,j_i l_i J_{F^{(s)}}} = \frac{\tilde{\gamma}^2_{\tau\,j_i l_i J_{F^{(s)}}}}{1 - \tilde{\gamma}^2_{\tau\,j_i l_i J_{F^{(s)}}}\,[\mathrm{d}S_{l_i}(E_{xA})/\mathrm{d}E_{xA}]\big|_{E_{xA}=E_\tau}}. \tag{15}$$

For the subthreshold resonance ($\tau = 1$) [51]

$$\frac{[C_{1\,j_i l_i J_{F^{(s)}}}]^2\,W^2_{-\,\eta^{(s)}_{xA},l_i+1/2}(2\,\kappa^{(s)}_{xA}\,R_{xA})}{2\,\mu_{xA}\,R_{xA}} = \frac{\gamma^2_{1\,j_i l_i J_{F^{(s)}}}}{1 + \gamma^2_{1\,j_i l_i J_{F^{(s)}}}\,[\mathrm{d}S_{l_i}(E_{xA})/\mathrm{d}E_{xA}]\big|_{E_{xA}=-\varepsilon^{(s)}_{xA}}} = \tilde{\gamma}^2_{1\,j_i l_i J_{F^{(s)}}}, \tag{16}$$

where $\tilde{\gamma}^2_{1\,j_i l_i J_{F^{(s)}}}$ and $\gamma^2_{1\,j_i l_i J_{F^{(s)}}}$ are the observed and formal reduced widths of the subthreshold resonance; $C_{1\,j_i l_i J_{F^{(s)}}}$ is the asymptotic normalization coefficient (ANC) of the subthreshold bound state $(x\,A)^{(s)}$ for the decay to the channel $(x + A)_{1\,j_i l_i J_{F^{(s)}}}$, $W_{-\eta^{(s)}_{xA},l_i+1/2}(2\,\kappa^{(s)}_{xA}\,R_{xA})$ is the Whittaker function, $\eta^{(s)}_{xA} = (Z_x\,Z_A/137)\mu_{xA}/\kappa^{(s)}_{xA}$ and $\kappa^{(s)}_{xA}$ are the $x - A$ Coulomb parameter and the bound-state wave number of the subthreshold bound state $F^{(s)}$, $\mu_{xA}$ is the reduced mass of $x$ and $A$, $Z_j\,e$ is the charge of nucleus $j$, $S_{l_i}(E_{xA})$ is the $R$-matrix Thomas shift function [55].

Now we return to the transfer reaction amplitude $M^{M_s\,M_{F^{(s)}_\tau}}_{M_a\,M_A\,\tau}(\mathbf{k}_{sF_\tau}, \mathbf{k}_{aA})$. To calculate it we use the three-body approach in which we neglect the internal degrees of freedom of particles $x$, $A$ and $s$. The potential $\overline{V}_{xA}(r_{xA})$ depends only on the distance between $x$ and $A$. Then the amplitude of the direct transfer reaction (5) in the plane-wave, surface-integral approximation reduces to [3, 8]

$$M^{M_s\,M_{F_\tau^{(s)}}}_{M_a\,M_A\,\tau}(\mathbf{k}_{sF_\tau},\mathbf{k}_{aA}) = \frac{\sqrt{\pi}}{\mu_{xA}}\,i^{l_i}\,\varphi_{sx}(p_{sx})\,R_{xA}\,\Upsilon_{\tau\,j_i l_i J_{F^{(s)}}}(R_{xA})\,\tilde{M}_{l_i}\sum_{M_x\,m_{j_i}\,m_{l_i}} < J_s\,M_s\;J_x\,M_x\big|J_a\,M_a >$$
$$\times < J_x\,M_x\;J_A\,M_A\big|j_i\,m_{j_i} >< j_i\,m_{j_i}\;l_i\,m_{l_i}\big|J_{F^{(s)}}\;M_{F_\tau^{(s)}} > Y^*_{l_i\,m_{l_i}}(\hat{\mathbf{p}}_{xA})$$
$$= \frac{\sqrt{\pi}}{\mu_{xA}}\,i^{l_i}\,\varphi_{sx}(p_{sx})\,\sqrt{2\,\mu_{xA}\,R_{xA}}\,\gamma_{\tau\,j_i l_i J_{F^{(s)}}}\tilde{M}_{l_i}\sum_{M_x\,m_{j_i}\,m_{l_i}} < J_s\,M_s\;J_x\,M_x\big|J_a\,M_a >$$
$$\times < J_x\,M_x\;J_A\,M_A\big|j_i\,m_{j_i} >< j_i\,m_{j_i}\;l_i\,m_{l_i}\big|J_{F^{(s)}}\;M_{F_\tau^{(s)}} > Y^*_{l_i\,m_{l_i}}(\hat{\mathbf{p}}_{xA}), \tag{17}$$

$$\tilde{M}_{l_i} = \left\{ j_{l_i}(p_{xA}\,R_{xA})\Big[B_{l_i}(k_{xA},\,R_{xA}) - 1 - D_{l_i}(p_{xA},\,R_{xA})\Big] + 2\mu_{xA}\frac{Z_x Z_A}{137}\int\limits_{R_{xA}}^{\infty} \mathrm{d}r_{xA}\,j_{l_i}(p_{xA}\,r_{xA})\frac{O_{l_i}(r_{xA})}{O_{l_i}(R_{xA})}\right\}, \tag{18}$$

$$D_{l_i}(p_{xA},\,R_{xA}) = R_{xA}\,\frac{\partial \ln j_{l_i}(p_{xA},r_{xA})}{\partial r_{xA}}\Big|_{r_{xA}=R_{xA}},\;\; B_{l_i}(k_{xA},\,R_{xA}) = R_{xA}\,\frac{\partial \ln O_{l_i}(k_{xA},r_{xA})}{\partial r_{xA}}\Big|_{r_{xA}=R_{xA}}. \tag{19}$$

Note that $M^{M_s\,M_{F_\tau^{(s)}}}_{M_a\,M_A\,\tau}(\mathbf{k}_{sF_\tau},\mathbf{k}_{aA})$ does not contain the hard-sphere scattering phase shift $\delta^{hs}_{l_i}$. Also, $\varphi_{sx}(p_{sx})$ is the Fourier transform of the radial part of the $s$-wave bound-state wave function $\varphi_{sx}(p_{sx})$ of the $a = (s\,x)$. Also, $\kappa_{sx} = \sqrt{2\,\mu_{sx}\,\varepsilon_{sx}}$ is the wave number of the bound-state $a = (s\,x)$, $\varepsilon_{sx}$ is its binding energy for the virtual decay $a \to s + x$. Since particles $s$ and $x$ are structureless, the spectroscopic factor of the bound state $a = (s\,x)$ is unity and we can use just the bound-state wave function $\varphi_{sx}$. In the center-off-mass of the reaction (2) $\mathbf{k}_{aA} = \mathbf{k}_a$, $\mathbf{k}_{sF_\tau} = \mathbf{k}_s$ and reviewpaper

$$\mathbf{p}_{xA} = \mathbf{k}_a - \frac{m_A}{m_F}\,\mathbf{k}_s, \qquad \mathbf{p}_{sx} = \mathbf{k}_s - \frac{m_s}{m_a}\,\mathbf{k}_a \tag{20}$$

are the off-shell $x - A$ and $s - x$ relative momenta in the vertices $x + A \to F_\tau$ and $a \to s + x$ of the diagram in Fig. 1, respectively, $\mathbf{p}_x = \mathbf{k}_a - \mathbf{k}_s$ is the off-shell momentum of the transferred virtual particle $x$, $\mathbf{k}_j$ is the on-shell momentum of particle $j$. Also $k_s$ and $E_{xA}$ are related by the energy conservation [3]:

$$E_{aA} - \varepsilon_{sx} = E_{xA} + k_s^2/(2\,\mu_{sF}), \tag{21}$$

where $\mu_{sF}$ is the reduced mass of particles $s$ and $F$.

Now we consider the amplitude $V_\nu$, $\nu = 1, 2$, describing the radiative decay of the intermediate resonance $F_\nu \to F + \gamma$ [56]:

$$V^{M_F\,M\,\lambda}_{M^{(s)}_{F_\nu}\,\nu} = -\int \mathrm{d}\mathbf{r}_{xA} < I^F_{xA}(\mathbf{r}_{xA})\,\big|\hat{\mathbf{J}}(\mathbf{r})\big|\Upsilon_\nu(\mathbf{r}_{xA}) > \cdot\mathbf{A}^*_{\lambda\,\mathbf{k}_\gamma}(\mathbf{r}), \tag{22}$$

where $I^F_{xA}(\mathbf{r}_{xA})$ is the overlap function of the bound-state wave functions of $x$, $A$ and the ground state of $F = (x\,A)$. Again, for the point-like nuclei $x$ and $A$ the overlap function $I^F_{xA}(\mathbf{r}_{xA})$ can be replaced by the single-particle bound-state wave function of $(xA)$ in the ground state. Also $\mathbf{A}^*_{\lambda\,\mathbf{k}_\gamma}(\mathbf{r})$ is the electromagnetic vector potential of the photon with helicity $\lambda = \pm 1$ and momentum $\mathbf{k}_\gamma$ at coordinate $\mathbf{r}_{xA}$. $\hat{\mathbf{J}}(\mathbf{r})$ is the charge current density operator. Matrix element in Eq. (22) is written assuming that on the first stage of the reaction the excited state $F_\nu$, $\nu = 1, 2$, is populated, which subsequently decays to the ground state $F$.

Using the multipole expansion of the vector potential, leaving only the electric components with the lowest allowed multipolarities $L$ and using the long wavelength approximation for $\hat{\mathbf{J}}(\mathbf{r})$, see for details [56], we get

$$V^{M_F\,M\,\lambda}_{M_{F^{(s)}_\nu}\,\nu} = -\frac{1}{2\,\pi}\sum_L \sqrt{\frac{1}{2\,k_\gamma}}\sqrt{\frac{L+1}{L}}\,\sqrt{\hat{J}_F\,\hat{l}_f}\,\frac{i^{-L}\,k_\gamma^L}{(2\,L-1)!!}\,e\,Z_{eff(L)}\left[D^L_{M\,\lambda}(\phi,\,\theta,0)\right]^*$$

$$\times\; <l_f\,0\;L\,0|l_i\,0> \;(-1)^{l_i-j_i-J^L_{F^{(s)}}}\; <J_F\,M_F\;L\,M|J^L_{F^{(s)}}\,M^L_{F^{(s)}_\nu}> \left\{\begin{array}{c} l_f\;j_i\;J_F \\ J^L_{F^{(s)}}\;L\;l_i\end{array}\right\} R^L_{\nu\,j_f\,l_f\,J_F\,j_i\,l_i\,J^L_{F^{(s)}}}$$

$$= \frac{\sqrt{2}}{4\,\pi}\sum_L i^{-L}\,(-1)^{L+1}\sqrt{\hat{L}}\,k_\gamma^{L-1/2}\,[\gamma^{J^L_{F^{(s)}}}_{(\gamma)\,\nu\,J_F\,L}]\left[D^L_{M\,\lambda}(\phi,\,\theta,0)\right]^*\,<J_F\,M_F\;L\,M|J^L_{F^{(s)}}\,M^L_{F^{(s)}_\nu}>, \qquad (23)$$

where $\gamma^{J^L_{F^{(s)}}}_{(\gamma)\,\nu\,J_F\,L}$ is the formal $R$-matrix radiative width amplitude for the electric $EL$ transition $J^L_{F^{(s)}} \to J_F$ given by the sum of the internal and external radiative width amplitudes, see Eqs (32) and (33) from [57], in which we singled out $\sqrt{2}\,k_\gamma^{L+1/2}$. Because now we take into account a few multipolarities $L$, we replace the previously introduced spin of the intermediate resonance $J_{F^{(s)}}$ by $J^L_{F^{(s)}}$, where the superscript $L$ denotes the multipolarity of the $EL$ transition to the ground state $F$. Replacement of $J_{F^{(s)}}$ by $J^L_{F^{(s)}}$ takes into account that the spins of the intermediate excited states are different for different multipolarities. Since we added the subscript $L$ to the spin of the intermediate resonance we added the same subscript to its projection $M^L_{F^{(s)}_\nu}$. It is important to note that $V^{M_F\,M\,\lambda}_{M_{F^{(s)}_\nu}\,\nu}$ does not depend on the hadr-sphere scattering phase shift.

The determined radiative width amplitude is related to the formal resonance radiative width by the standard equation

$$\Gamma^{J^L_{F^{(s)}}}_{(\gamma)\,\nu\,J_F\,L} = 2\,k_\gamma^{L+1/2}\,(\gamma^{J^L_{F^{(s)}}}_{(\gamma)\,\nu\,J_F\,L})^2. \qquad (24)$$

Note that the observable radiative width is related to the formal one by

$$(\tilde{\gamma}^{J^L_{F^{(s)}}}_{(\gamma)\,\nu\,J_F\,L})^2 = \frac{(\gamma^{J^L_{F^{(s)}}}_{(\gamma)\,\nu\,J_F\,L})^2}{1+\gamma^2_{\nu\,j_i l_i J_{F^{(s)}}}\left[\mathrm{d}S_{l_i}(E_{xA})/\mathrm{d}E_{xA}\right]\big|_{E_{xA}=E_\nu}}. \qquad (25)$$

We consider the two-level approach with $\nu = 1$ ($\nu = 2$) corresponding to the subthreshold resonance (the resonance at $E_{xA} > 0$). Then $E_\nu = -\varepsilon^{(s)}_{xA}$ for $\nu = 1$ and $E_\nu = E_R$ for $\nu = 2$ with $E_R$ being the resonance energy corresponding to the level $\nu = 2$. This observable radiative width is related to the observable resonance radiative width as

$$\tilde{\Gamma}^{J^L_{F^{(s)}}}_{(\gamma)\,\nu\,J_F\,L} = 2\,k_\gamma^{L+1/2}\,(\tilde{\gamma}^{J^L_{F^{(s)}}}_{(\gamma)\,\nu\,J_F\,L})^2. \qquad (26)$$

Also in Eq. (23) $M$ is the projection of the angular momentum $L$ of the emitted photon (multipolarity of the electromagnetic transition), $e\,Z_{eff(L)}$ is the effective charge of the $x+A$ system for the electric transition $EL$. The matrix element $R^L_{\nu j_f\,l_f\,J_F\,j_i\,l_i\,J^L_{F^{(s)}}}$ is

$$R^L_{\nu j_f\,l_f\,J_F\,j_i\,l_i\,J^L_{F^{(s)}}} = < r^{L+2}_{xA} I_{j_i\,l_f\,J_F}(r_{xA})\Upsilon_{\nu\,j_i\,l_i\,J^L_{F^{(s)}}}(r_{xA})> . \qquad (27)$$

$\Upsilon_{\nu\,j_i\,l_i\,J^L_{F^{(s)}}}(r_{xA})$ is the resonant scattering wave function in the $R$-matrix approach whose external part is given by Eq. (9). Again, it follows from Eqs. (9) and (10) that $\Upsilon_{\nu\,j_i\,l_i\,J^L_{F^{(s)}}}(r_{xA})$ does not depend on the $R$-matrix hard-sphere scattering phase shift.

The internal resonant wave function $X_{int\,\tau}$ in the $R$-matrix approach matches the external one on the border $r_{xA} = R_{xA}$ and satisfies the boundary condition

$$X_{int\,\tau}(k_{xA},\,R_{xA}) = \sqrt{2\,\mu_{xA}\,R_{xA}}\,\gamma_{\tau\,j_i l_i J^L_{F^{(s)}}}. \qquad (28)$$

For $\tau = 1$ $X_{int\,1}$ is the overlap function of the bound-state wave functions of $F^{(s)} = (x\,A)^{(s)}$, $x$ and $A$, which is normalized to untiy over the internal region $r_{xA} \le R_{xA}$.

Substituting Eqs. (17) and (23) into Eq. (4) we get the expression for the indirect reaction amplitude

$$M^{M_s\ M_F\ M\,\lambda}_{M_a\ M_A} = \frac{\varphi_{sx}(p_{sx})}{2}\sqrt{\frac{R_{xA}}{\pi\,\mu_{xA}}}\sum_{L}(-1)^{L+1}\,\hat{L}^{1/2}\,k_\gamma^{L-1/2}\left[D^L_{M\,\lambda}(\phi,\,\theta,0)\right]^*\sum_{l_i} i^{l_i-L}\,\tilde{M}_{l_i}$$

$$\times\sum_{\nu,\,\tau=1}^{2}\gamma^{J^L_{F^{(s)}}}_{(\gamma)\,\nu\,J_F\,L}\,\mathbf{A}^L_{\nu\,\tau}\,\gamma_{\tau\,j_i l_i J^L_{F^{(s)}}}\sum_{M^L_{F^{(s)}_\nu}} < J_F\,M_F\ L\,M\big|J^L_{F^{(s)}}\,M^L_{F^{(s)}_\nu}>$$

$$\times\sum_{m_{j_i}\,m_{l_i}\,M_x} < j_i\,m_{j_i}\ l_i\,m_{l_i}\big|J^L_{F^{(s)}}\,M^L_{F^{(s)}_\tau}>< J_x\,M_x\ J_s\,M_s\big|J_a\,M_a>< J_x\,M_x\ J_A\,M_A\big|j_i\,m_{j_i}> Y^*_{l_i\,m_{l_i}}(\hat{\mathbf{p}}_{xA}). \qquad (29)$$

The amplitude $M^{M_s\ M_F\ M\,\lambda}_{M_a\ M_A}$ describes the indirect reaction proceeding through the intermediate resonances, which decay to the ground state $F=(x\,A)$ by emitting photons. Equation (29) is generalization of Eq. (4) by including the sum over multipolarities $L$ corresponding to the radiative electric transitions from the intermediate resonances with the spins $J^L_{F^{(s)}}$ to the ground state $F$ with the spin $J_F$. Note also that we assume that two levels contribute to each transition of multipole $L$. It requires the two-level generalized $R$-matrix approach. The generalization of Eq. (29) for three- or more-level cases is straightforward. In Eq. (29) the reaction part and radiative parts are interconnected by the $R$-matrix level matrix elements $\mathbf{A}^L_{\nu\,\tau}$. Note that $M^{M_s\ M_F\ M\,\lambda}_{M_a\ M_A}$ does not contain the $R$-matrix hard-sphere scattering phase shift.

The part $\sum_{\nu,\,\tau=1}^{2}\gamma^{J^L_{F^{(s)}}}_{(\gamma)\,\nu\,J_F\,L}\,\mathbf{A}^L_{\nu\,\tau}\,\gamma_{\tau\,j_i l_i J^L_{F^{(s)}}}$ is the standard $R$-matrix term for the binary resonant radiative capture reaction. However, we analyze the three-body reaction $a(x\,s)+A\to s+F+\gamma$ with the spectator $s$ in the final state rather than the standard two-body radiative capture reaction $x+A\to F+\gamma$. This difference leads to the generalization of the standard $R$-matrix approach for the three-body reactions resulting in the appearance of the additional terms, $\varphi_{sx}(p_{sx})\,\tilde{M}_{l_i}$. That is why we call the developed approach the generalized $R$-matrix method for the indirect resonant radiative capture reactions.

(i) The most important feature of this approach is that the indirect reaction amplitude does not contain the penetrability factor $P_{l_i}(E_{xA},R_{xA})$ in the entry channel of the sub-reaction (2). This factor is the main obstacle to measure the astrophysical factor of this reaction if one uses direct measurements. The absence of this penetrability factor in the entry channel of the sub-reaction allows one to use the indirect method to get the information about the astrophysical factor of the sub-reaction.
(ii) The indirect reaction amplitude is parameterized in terms of the formal $R$-matrix width amplitudes, which are connected to the observable resonance widths.
(iii) The final expression for the indirect reaction amplitude $M^{M_s\ M_F\ M\,\lambda}_{M_a\ M_A}$ does not depend on the $R$-matrix hard-sphere scattering phase shift.

We take the indirect reaction amplitude at fixed projections of the spins of the initial and final particles including the fixed projection $M$ of the orbital momentum $L$ of the emitted photon and fixed its chirality $\lambda$. For example, for the $^{12}$C$(\alpha,\,\gamma)^{16}$O reaction the electric dipole $E1$ ($L=1$) and quadrupole $E2$ ($L=2$) transitions do contribute and they interfere. In the long wavelength approximation only minimal allowed $l_i$ for given $L$ does contribute. For example, for the case considered below $l_f=0\ \ l_i=L=1$ for the dipole and $l_i=L=2$ for the quadrupole electric transitions do contribute. The dimension of the $R$-matrix level matrix $\mathbf{A}^L$ depends on the number of the levels taken into account for each $L$.

The indirect reaction amplitude depends on the off-shell momenta $\mathbf{p}_{sx}$ and $\mathbf{p}_{xA}$. Both off-shell momenta are expressed in terms of $\mathbf{k}_a$ and $\mathbf{k}_s$, see Eq. (20). Also the the indirect reaction amplitude depends on the momentum of the emitted photon $\mathbf{k}_\gamma$ whose direction is determined by the angles in the Wigner $D$-function.

In the center-off-mass of the reaction (3) neglecting the recoil effect of the nucleus $F$ during the photon emission from the energy conservation we get

$$E_{aA}+Q=E_{sF}+k_\gamma, \qquad (30)$$
$$k_\gamma=E_{xA}+\varepsilon_{xA}, \qquad (31)$$

where $E_{sF}=k_s^2/(2\,\mu_{sF})$, $Q=\varepsilon_{xA}-\varepsilon_{sx}$ and $\varepsilon_{xA}$ is the binding energy of the ground state of the nucleus $F$.

To estimate the recoil effect we take into account that in the center-off-mass of the reaction (3) the momentum conservation in the final state gives

$$\mathbf{k}^{'}_F=-\mathbf{k}_\gamma-\mathbf{k}_s, \qquad (32)$$

where $\mathbf{k}^{'}_F$ is the momentum of the final nucleus $F$ after emitting the photon. Then the energy conservation leads to

$$E_{aA}-\varepsilon_{sx}=\frac{k_s^2}{2\,\mu_{sF}}+E_{xA}=\frac{k_s^2}{2\,m_s}+\frac{(k^{\prime}_F)^2}{2\,m_F}+k_\gamma \qquad (33)$$
$$=\frac{k_s^2}{2\,\mu_{sF}}+2\frac{k_s\,k_\gamma}{2\,m_F}\cos\theta^{\prime}+\frac{k_\gamma^2}{2\,m_F}+k_\gamma. \qquad (34)$$

We remind that we use the system of units in which $\hbar=c=1$, that is, $E_\gamma=k_\gamma$. Evidently that the term $\frac{k_\gamma^2}{2\,m_F}=E_\gamma\,\frac{E_\gamma}{2\,m_F}$ can be neglected because $E_\gamma<<m_F$.

The contribution of the term $2\frac{k_s\,k_\gamma}{2\,m_F}\cos\theta'$ depends on $\cos\theta' = \hat{\mathbf{k}}_s\cdot\hat{\mathbf{k}}_\gamma$.

To estimate the recoil effect of the nucleus $F$ we consider the reaction $^{12}$C($^6$Li, $d\,\gamma$)$^{16}$O at the most effective astrophysical energy $E_{xA} = E_{\alpha\,^{12}\mathrm{C}} = 0.3$ MeV; the energy of the emitted photon is $k_\gamma \approx 7$ MeV and $E_{aA} = 7$ MeV. As we will see below (Fig. (4)) at 0.3 MeV the maximum of the photon's angular distribution is at $\theta = 52^\circ$, where $\theta$ is the angle between $\mathbf{p}_{\alpha\,^{12}\mathrm{C}}$ and $\mathbf{k}_\gamma$. In the QF kinematics $\mathbf{p}_{\alpha\,^{12}\mathrm{C}}||\mathbf{k}_d$ where $\mathbf{k}_s = \mathbf{k}_d$, that is, $\theta' = \theta$. At $\theta = 52^\circ$, which is the maximum of the photon's angular distribution and is close to the maximum of the angular distribution for the $E2$ transition, the recoil effect is $\sim 6.5\%$. Note that for the $E1$ transition the photon's angular distribution has a peak at $90^\circ$ at which the recoil effect vanishes.

Neglecting the recoil effect of the nucleus $F$ in Eq. (33) we can replace $k_F^{'}$ by $k_s$. Then $k_\gamma$ and $k_s$ are related by Eq. (30) while $k_\gamma$ and $E_{xA}$ are related by Eq. (31). If we would take into account the recoil effect then the relationship between $k_\gamma$ and $E_{xA}$ is more complicated then Eq. (31) and is given by

$$k_\gamma = \frac{E_{xA}}{\frac{k_s\,\cos\theta'}{m_F}+1}, \tag{35}$$

where we neglected the extremely small term $\frac{k_\gamma^2}{2\,m_F}$. However, in this paper, because we don't analyze the real data and make a proposal, we neglect the recoil effect of the nucleus $F$.

The expression for $p_{xA}$ is needed to calculate $\tilde{M}_{l_i}$. From the energy-momentum conservation law in the three-ray vertices $a \to s + x$ and $x + A \to F^{(s)}$ of the diagram in Fig. 1 we get [3]

$$E_{xA} = \frac{p_{xA}^2}{2\,\mu_{xA}} - \frac{p_{sx}^2}{2\,\mu_{sx}} - \varepsilon_{s\,x}. \tag{36}$$

In the QF kinematics $p_{sx} = 0$ and

$$E_{xA} = \frac{p_{xA}^2}{2\,\mu_{xA}} - \varepsilon_{s\,x}. \tag{37}$$

Thus always $\frac{p_{xA}^2}{2\,\mu_{xA}} > E_{xA}$.

## III. DIFFERENTIAL CROSS SECTIONS

### A. Triple differential cross section

Let us consider the indirect resonant reaction contributed by different interfering multipoles $L$. For each $L$ we assume two-level contribution. Then the triple differential cross section of the resonant indirect radiative capture reaction for unpolarized initial and final particles (including the photon) in the center-off-mass of the reaction (3) is given by

$$\frac{\mathrm{d}\sigma}{\mathrm{d}\Omega_{\hat{\mathbf{k}}_s}\,\mathrm{d}\Omega_{\hat{\mathbf{k}}_\gamma}\,\mathrm{d}E_{sF}} = \frac{\mu_{aA}\,\mu_{sF}}{\hat{J}_a\,\hat{J}_A(2\,\pi)^5}\,\frac{k_{sF}\,k_\gamma^2}{k_{aA}}\sum_{M_a\,M_A\,M_s\,M_F\,M\,\lambda}\left|M_{M_a\,M_A}^{M_s\,M_F\,M\,\lambda}\right|^2$$

$$= -\frac{1}{(2\,\pi)^7}\,\frac{\mu_{aA}\,\mu_{sF}}{\hat{J}_x\,\hat{J}_A}\,\frac{\varphi_{sx}^2(p_{sx})\,R_{xA}}{4\,\mu_{xA}}\,\frac{k_{sF}}{k_{aA}}\,(-1)^{J_F-j_i}\sum_{L'\,L}(-1)^{L'+L}\,k_\gamma^{L'+L+1}\;\hat{J}_{F^{(s)}}^{L'}\,\hat{J}_{F^{(s)}}^{L}\,\sqrt{\hat{L}'\,\hat{L}}\sum_{l_i'\,l_i\,l} i^{L'-l_i'-L+l_i}\,\sqrt{\hat{l}_i'\,\hat{l}_i}$$

$$\times\;\tilde{M}_{l_i'}^*\,\tilde{M}_{l_i}\left\{\begin{array}{cc} j_i\,l_i'\,J_{F^{(s)}}^{L'} \\ l\,J_{F^{(s)}}^{L}\,l_i\end{array}\right\}\left\{\begin{array}{ccc} J_{F^{(s)}}^{L'}\,J_F\,L' \\ L\,l\,J_{F^{(s)}}^{L}\end{array}\right\}\sum_{\nu',\,\nu,\,\tau',\,\tau=1}^{2}\left[\gamma_{(\gamma)\,\nu'\,J_F\,L'}^{J_{F^{(s)}}^{L'}}\right]^*\left[\gamma_{(\gamma)\,\nu\,J_F\,L}^{J_{F^{(s)}}^{L}}\right]\left[\mathbf{A}_{v'\,\tau'}^{L'}\right]^*\left[\mathbf{A}_{\nu\,\tau}^{L}\right]$$

$$\times,\gamma_{\tau'\,j_i l_i' J_{F^{(s)}}^{L'}}\;\gamma_{\tau\,j_i l_i J_{F^{(s)}}^{L}} < l_i'0\;l_i\,0\big|l\,0><L'1\;L\;-1\big|l\,0>\;[1+(-1)^{L'+L+l}]\,P_l(cos\theta). \tag{38}$$

To obtain Eq. (38) we adopted $z\,||\,\hat{\mathbf{p}}_{xA}$, that is, $Y_{l\,m_l}(\hat{\mathbf{p}}_{xA}) = \sqrt{\frac{\hat{l}}{4\,\pi}}\,\delta_{m_l\,0}$. Thus, in the plane-wave approximation, the direction $\hat{\mathbf{p}}_{xA}$ becomes the axis of the symmetry. Note that if we replace the plane waves by the distorted waves, the vestige of this symmetry will still survive [12].

We remind that the radiative transition $J_{F^{(s)}}^L \to J_F$ is the electric $EL$ where $J_{F^{(s)}}^L$ is the spin of the intermediate state (subthreshold resonance or resonance).

For a more simple case when only one multipole $L$ contributes into the radiative transition, the triple differential cross section takes the form:

$$\frac{\mathrm{d}\sigma}{\mathrm{d}\Omega_{\hat{\mathbf{k}}_s}\,\mathrm{d}\Omega_{\hat{\mathbf{k}}_\gamma}\,\mathrm{d}E_{sF}} = -\frac{1}{(2\,\pi)^7}\,\frac{\mu_{aA}\,\mu_{sF}}{\hat{J}_x\,\hat{J}_A}\,\frac{\varphi^2_{sx}(p_{sx})\,R_{xA}}{2\,\mu_{xA}}\,\frac{k_{sF}}{k_{aA}}\,k_\gamma^{\hat{L}}\,(-1)^{J_F-j_i}\,\hat{L}\,(\hat{J}^L_{F^{(s)}})^2\sum_{l_i\,l}\hat{l}_i$$
$$\times\,\big|\tilde{M}_{l_i}\big|^2\left\{\begin{array}{cc} j_i\,l_i\,J^L_{F^{(s)}} \\ l\,J^L_{F^{(s)}}\,l_i\end{array}\right\}\left\{\begin{array}{cc} J^L_{F^{(s)}}\,J_F\,L \\ L\,l\,J^L_{F^{(s)}}\end{array}\right\}\sum_{\nu',\,\nu,\,\tau',\,\tau=1}^{2}\big[\gamma^{J^L_{F^{(s)}}}_{(\gamma)\,\nu'\,J_F\,L}\big]^*\big[\gamma^{J^L_{F^{(s)}}}_{(\gamma)\,\nu\,J_F\,L}\big]\,\big[\mathbf{A}^L_{\upsilon'\,\tau'}\big]^*\,\big[\mathbf{A}^L_{\nu\,\tau}\big]$$
$$\times,\gamma_{\tau'\,j_i l_i J^L_{F^{(s)}}}\,\gamma_{\tau\,j_i l_i J^L_{F^{(s)}}}\,<l_i\,0\;l_i\,0\big|l\,0><L\,1\;L\;-1\big|l\,0>\,P_l(cos\theta). \qquad (39)$$

Also formally we keep the summation over $l_i$, in the long wavelength approximation for given $L$ at astrophysically relevant energies only minimal allowed $l_i$ does contribute.

The triple differential cross section depends on $\mathbf{k}_s$ and $\mathbf{k}_\gamma$. Because we neglected the recoil of the final nucleus $F$, $k_s$ and $k_\gamma$ are related by Eq. (30). We remind that we selected axis $z||\mathbf{p}_{xA}$. Hence the photon's scattering angle is counted from $\mathbf{p}_{xA}$, which itself is determined by $\mathbf{k}_s$. Thus the angular dependence of the triple differential cross section determines the angular correlation between the emitted photons from the intermediate excited state $F^*$ and the spectator $s$. Because we consider the three-body reaction (3) the angular correlation function also depends on the spins $J^L_{F^{(s)}}$ of the intermediate nucleus $F^*$ which decays to $F$.

By choosing QF kinematics, $p_{sx}=0$, one can provide the maximum of the triple differential cross section due to the maximum of $\varphi^2_{sx}(p_{sx})$. At fixed $\mathbf{k}_s$ the triple differential cross section determines the emitted photon's angular distribution, which is contributed by different interfering multipoles $L$. By measuring the photon's angular distributions at different photon's energies (that is, at different $k_s$ or $E_{xA}$) one can determine the energy dependence of the photon's angular distribution. However, a wide variation of $\mathbf{k}_s$ away from the QF kinematics $\mathbf{p}_{sx}=\mathbf{k}_s-(m_s/m_a)\,\mathbf{k}_a=0$ will decrease the differential cross section due to the drop of $\varphi^2_{sx}(p_{sx})$. Usually, in indirect methods $\mathbf{k}_s$ is varied in the interval in which $p_{sx}\leq\kappa_{sx}$ [3].

### B. Double differential cross section

Integrating the triple differential cross section over the the photon's solid angle $\Omega_{\hat{\mathbf{k}}_\gamma}$ we get the non-coherent sum of the double differential cross sections with different multipoles $L$:

$$\frac{\mathrm{d}\sigma}{\mathrm{d}\Omega_{\hat{\mathbf{k}}_s}\,\mathrm{d}E_{sF}} = \frac{1}{(2\,\pi)^6}\,\frac{\mu_{aA}\,\mu_{sF}}{\hat{J}_x\,\hat{J}_A}\,\frac{\varphi^2_{sx}(p_{sx})\,R_{xA}}{\mu_{xA}}\,\frac{k_{sF}}{k_{aA}}\sum_L\sqrt{\hat{L}\,\hat{J}^L_{F^{(s)}}}\,k_\gamma^{\hat{L}}\sum_{l_i}\big|\tilde{M}_{l_i}\big|^2$$
$$\times\sum_{\nu',\,\nu,\,\tau',\,\tau=1}^{2}\big[\gamma^{J^L_{F^{(s)}}}_{(\gamma)\,\nu'\,J_F\,L}\big]^*\big[\gamma^{J^L_{F^{(s)}}}_{(\gamma)\,\nu\,J_F\,L}\big]\,\big[\mathbf{A}^L_{\upsilon'\,\tau'}\big]^*\,\big[\mathbf{A}^L_{\nu\,\tau}\big]\;\gamma_{\tau'\,j_i\,l_i\,J^L_{F^{(s)}}}\,\gamma_{\tau\,j_i\,l_i\,J^L_{F^{(s)}}}. \qquad (40)$$

Despite of the virtual transferred particle $x$ in the diagram of Fig. 1, using the surface integral approach and the generalized $R$-matrix we can rewrite the double differential cross section in terms of the on-the-energy-shell (OES) astrophysical factor for the resonant radiative capture $A(x,\,\gamma)F$ for the electric transition of the multipolarity $L$ and the relative orbital angular momentum $l_i$ of particles $x$ and $A$ in the entry channel of the $A(x,\,\gamma)F$ raiative capture. In the $R$-matrix formalism this astrophysical factor is given by [5]

$$S_{EL,l_i}(E_{xA})(MeVb) = 2\,\pi\,\lambda_N^2\,\frac{\hat{J}^L_{F^{(s)}}}{\hat{J}_x\,\hat{J}_A}\,\frac{1}{\mu_{xA}}\,m_N^2\,e^{2\,\pi\,\eta_i}\,P_{l_i}(E_{xA},\,R_{xA})\,10^{-2}\,k_\gamma^{\hat{L}}\left|\sum_{\nu,\tau}\big[\gamma^{J^L_{F^{(s)}}}_{(\gamma)\,\nu\,J_F\,L}\big]\,\big[\mathbf{A}^L_{\nu\,\tau}\big]\;\gamma_{\tau\,j_i\,l_i\,J^L_{F^{(s)}}}\right|^2. \qquad (41)$$

Here, $\lambda_N=0.2118$ fm is the Compton nucleon wave length, $m_N=931.5$ MeV is the atomic mass unit, $\mu_{xA}$ is

the $x-A$ reduced mass expressed in MeV, $\eta_i$ is the $x-A$ Coulomb parameter at relative enerrgy $E_{xA}$. Then the indirect double differential cross section takes the form:

$$\frac{\mathrm{d}\sigma}{\mathrm{d}\Omega_{\hat{\mathbf{k}}_s}\,\mathrm{d}E_{sF}} = KF\,\varphi^2_{sx}(p_{sx})\,R_{xA}\sum_L\sqrt{\frac{\hat{L}}{\hat{J}^L_{F^{(s)}}}}\sum_{l_i}e^{-2\,\pi\,\eta_i}\,P^{-1}_{l_i}(E_{xA},\,R_{xA})\left|\tilde{M}_{l_i}\right|^2 S_{EL,l_i}(E_{xA}), \tag{42}$$

where

$$KF = \frac{10^2}{(2\,\pi)^7}\,\frac{\mu_{aA}\,\mu_{sF}}{m^2_N\,\lambda^2_N}\,\frac{k_{sF}}{k_{aA}} \tag{43}$$

is the kinematical factor.

To determine the astrophysical factor from the indirect double differential cross section we need to identify the region where accurate direct data are available and only one resonance dominates with given $L$ and $l_i$. By normalizing in this region the astrophysical factor obtained from the indirect measurement to the experimental one we get the

$$S_{EL,l_i}(E_{xA}) = NF\,\frac{\mathrm{d}\sigma}{\mathrm{d}\Omega_{\hat{\mathbf{k}}_s}\,\mathrm{d}E_{sF}}\sqrt{\frac{\hat{J}^L_{F^{(s)}}}{\hat{L}}}\,\frac{1}{KF\,\varphi^2_{sx}(p_{sx})\,R_{xA}}\,e^{2\,\pi\,\eta_i}\,P_{l_i}(E_{xA},\,R_{xA})\left|\tilde{M}_{l_i}\right|^{-2}. \tag{44}$$

Here, $NF$ is an energy-independent normalization factor providing correct astrophysical factor $S_{EL,l_i}(E_{xA})$ at higher energies. Using this normalization factor we can determine with accuracy, which is not achievable in any direct approach, the astrophysical factors at energies $E_{xA}\to 0$. This is the main achievement of the indirect approach. We remind that in our formalism we use the plane wave approximation rather than the distorted wave. But it should not affect the accuracy of our method because the distorted waves and plane wave approximation give similar energy dependence of the transfer reaction cross section. The normalization factor $NF$ compensates the inaccuracy of the plane wave approximation.

We summarize the methodology of the indirect method to obtain the astrophysical factor.
(1) Measurements of the photon's angular distribution (photon-spectator angular correlation) at different $E_{xA}$ energies covering the interval from low energies relevant to nuclear astrophysics up to higher energy at which direct data are available. To cover a broad energy range at fixed energy of the projectile, the energy, and scattering angle of the spectator should be varied near the QF kinematics ($p_{sx}=0$).
(2) Obtaining the indirect double differential cross section by integrating the triple differential cross section over the photon's scattering angle.
(3) Expressing the astrophysical factor in terms of the indirect double differential cross section.
(4) Normalization of astrophysical factor to the available experimental data at higher energy.
(5) Determination of the astrophysical factor at astrophysical energies.

## IV. RADIATIVE CAPTURE $^{12}$C$(\alpha,\,\gamma)^{16}$O VIA INDIRECT REACTION $^{12}$C$(^6\mathrm{Li},d\,\gamma)^{16}$O

In this section we demonstrate the application of the developed formalism for the analysis of the indirect reaction $^{12}$C$(^6\mathrm{Li},d\,\gamma)^{16}$O to obtain the information about the astrophysical factor for the $^{12}$C$(\alpha,\,\gamma)^{16}$O at energies $<1$ MeV. For our analysis we use the energy levels from [58].

At low energies the astrophysical reaction under consideration is contributed by the $L=1$ and $L=2$ electric transitions [24, 27, 29, 32, 37]. $E1$ transition to the ground state $J_F=0$, $l_f=0$ proceeds as the resonant capture through the wing at $E_{\alpha\,^{12}\mathrm{C}}>0$ of the subthreshold bound state $1^-$ at $E_{\alpha\,^{12}\mathrm{C}}=-0.045$ MeV, which works as the subthreshold resonance. Besides, the $E1$ transition to the ground state is contributed by the resonant capture through the low-energy tail of the $1^-$ resonance located at $E_R=2.423$ MeV. The $E2$ transition is contributed by the subthreshold $2^+$ state at $E_{\alpha\,^{12}\mathrm{C}}=-0.2449$ MeV and low-energy tail of $2^+$ resonance at 2.68 MeV.

These four states are observable physical states contributing to the low-energy radiative capture under consideration. Besides these states, when fitting the data the

artificial level was added for $E1$ transition (see, for example, [24, 27, 29, 32, 38] and references therein). In the present paper we calculate the photon's angular distribution (the angular photon-deuteron correlation) at low energies down to the most effective astrophysical energy $E_{\alpha\,^{12}\mathrm{C}} = 0.3$ MeV.

We take into account the mentioned four physical states and added one artificial state for the $E1$ transition. It can be explained qualitatively why the background level is necessary to include into the fit of the $E1$ transition. The problem is that the subthreshold state $J = 1$, $E_{\alpha\,^{12}\mathrm{C}} = -0.045$ MeV and the resonance $J = 1$, $E_R = 2.423$ MeV cannot decay by the $E1$ transition to the ground state of $^{16}$O because all of them have the isospin $T = 0$. Evidently that the observed weak $E1$ transition from the first two $J = 1$, $T = 0$ states is possible only due to the small admixture of the higher lying $J = 1$, $T = 1$ states [19].

The reduced widths of the subthreshold resonances are known from the experimental ANCs [27, 43] and the reduced width of the $1^-$, 2.423 MeV resonance is determined from the resonance width. We disregard the cascade transitions to the ground state of $^{16}$O through subthreshold states. According to [19], the sum of all cascade transitions contributes only $7 - 10\%$. Because we don't pursue here a perfect fit, we neglect all the cascade transitions. In our fit, as in Ref. [20], we also disregard the $E2$ direct radiative capture to the ground state $^{16}$O.

For the case under consideration $J_x = 0$, $J_A = 0$, $j_i = 0$, $l_i = L = J^L_{F(s)}$, $J_F = 0$ and the expression for the triple differential cross section for the case under consideration simplifies to

$$\frac{\mathrm{d}\sigma}{\mathrm{d}\Omega_{\hat{\mathbf{k}}_s}\,\mathrm{d}\Omega_{\hat{\mathbf{k}}_\gamma}\,\mathrm{d}E_{sF}} = -\frac{\mu_{aA}\,\mu_{sF}}{(2\,\pi)^7}\,\frac{\varphi^2_{sx}(p_{sx})\,R_{xA}}{2\,\mu_{xA}}\,\frac{k_{sF}}{k_{aA}}\sum_{L'\,L}(-1)^{L'+L}\,k_\gamma^{L'+L+1}\,\sqrt{\hat{L}'\,\hat{L}}$$
$$\times\ \tilde{M}^*_{L'}\,\tilde{M}_L\sum_{\nu',\,\nu,\,\tau',\,\tau=1}^{2}\left[\gamma^{L'}_{(\gamma)\,\nu'\,0\,L'}\right]^*\left[\gamma^{L}_{(\gamma)\,\nu\,0\,L}\right]\left[\mathbf{A}^{L'}_{\nu'\,\tau'}\right]^*\left[\mathbf{A}^{L}_{\nu\,\tau}\right]$$
$$\times,\gamma_{\tau'\,0\,L'\,L'}\,\gamma_{\tau\,0\,L\,L}\sum_{l} < L'\,0\ L\,0\big|l\,0 >< L'\,1\ L\ -1\big|l\,0 >\ P_l(cos\theta). \tag{45}$$

Here, $a = {}^6$Li, $A = {}^{12}$C, $s = d$, $x = \alpha$, $F = {}^{16}$O. This expression is used for the analysis of the indirect reaction $^{12}\mathrm{C}(^6\mathrm{Li}, d\,\gamma)^{16}\mathrm{O}$ at low energies. We outline here some details of the calculations.

After integration over the photon's solid angle we get the indirect double differential cross section (42) in which $l_i = L$. Then at energies near the $1^-$ resonance at 2.423 MeV where, as we will see below, the $E1$ transition completely dominates,

$$S_{E1}(E_{xA}) = NF\,\frac{\mathrm{d}\sigma}{\mathrm{d}\Omega_{\hat{\mathbf{k}}_s}\,\mathrm{d}E_{sF}}\,\frac{1}{KF\,\varphi^2_{sx}(p_{sx})\,R_{xA}}\,e^{2\,\pi\,\eta_i}\,P_1(E_{xA},\,R_{xA})\left|\tilde{M}_1\right|^{-2}. \tag{46}$$

The $S(E1)$ astrophysical factor was measured at energies near 2.423 MeV with a very good accuracy [19, 32, 36]. Should we have the experimental indirect double differential cross section expressed in arbitrary units, we can use Eq. (46) to normalize the $S_{E1}(E_{xA})$ to the experimental one at higher energies. After that, having measured indirect double differential cross section at 0.3 MeV, we can determine the $S_{E1}(0.3\mathrm{MeV}) + S_{E2}(0.3\mathrm{MeV})$.

In this paper we calculate the photon's angular distribution at different $E_{\alpha\,^{12}\mathrm{C}}$ energies for the $^{12}\mathrm{C}(\alpha, d\,\gamma)^{16}\mathrm{O}$ reaction and how it is affected by the interference character (constructive or destructive) of the $1^-$ subthreshold bound state and $1^-$ resonance. In the $R$-matrix approach the fitting parameters are the formal reduced widths which are related to the observable ones by Eq. (15). The observable reduced widths $(\tilde{\gamma}_{1\,0\,1\,1})^2$ and $(\tilde{\gamma}_{1\,0\,2\,2})^2$ are expressed in terms of the corresponding ANCs of the subthreshold bound states by Eq. (16). For the ANCs of the $1^-$ and $2^+$ subthreshold states we adopted $[C^{(s)}_{(\alpha\,^{12}\mathrm{C})1}]^2 = 4.39\times10^{28}$ fm$^{-1}$ and $[C^{(s)}_{(\alpha\,^{12}\mathrm{C})2}]^2 = 1.48\times10^{10}$ fm$^{-1}$ [43], respectively. In all the calculations, following [27], we use the channel radius $R_{\alpha\,^{12}\mathrm{C}} = 6.5$ fm. The observable reduced width of the resonance $1^-$ is expressed in terms of the observable resonance width of this resonance. For this resonance we adopt $\tilde{\Gamma}_{2\,011} = 0.48$ MeV [58]. In the case under consideration for the $E1$ transition we take into account three states and select the boundary con-

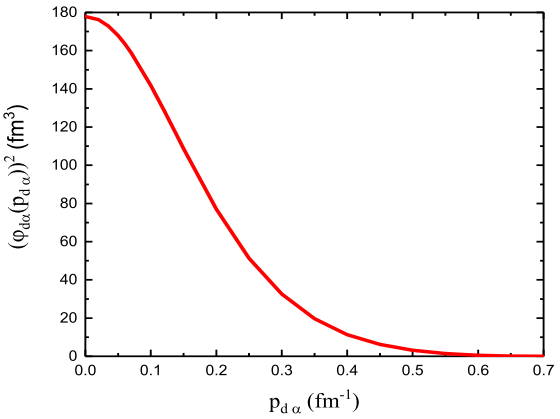


FIG. 2: Square of the $d-\alpha$ bound state wave function in the momentum space.

dition at the energy of the first level, which is the $1^-$ subthreshold bound state, that is, $E_1 = -\varepsilon^{(s)}_{xA(1)}$.

For the $E2$ transition we take into account two levels and select the boundary condition at the energy of the $2^+$ subthreshold bound state $E_2 = -0.245$ MeV.

Now we discuss the radiative width amplitudes. We use Eq. (25) to express the formal radiative widths amplitudes $\gamma^1_{(\gamma)\,1\,0\,1}$, $\gamma^1_{(\gamma)\,2\,0\,1}$ and $\gamma^2_{(\gamma)\,1\,0\,2}$ in terms of corresponding observable reduced widths, which are related to the observable radiative resonance widths by Eq. (26) [55].

Another important point to discuss is the kinematics of the indirect reaction. The triple differential cross section is proportional to $\varphi^2_{d\,\alpha}(p_{d\,\alpha})$, which is shown in Fig. 2. The maximum of $\varphi^2_{d\,\alpha}(p_{d\,\alpha})$ at $p_{d\,\alpha} = 0$ (QF kinematics) also provides the maximum of the triple differential cross section. $p_{d\,\alpha}$ is the $d-\alpha$ relative momentum in the three-ray vertex ${}^6\mathrm{Li} \to d + \alpha$ of the diagram in Fig. 1.

To calculate the Fourier transform of the ${}^6\mathrm{Li} = (d\,\alpha)$ bound-state wave function we use the Woods-Saxon potential with the depth $V_0 = 60.0$ MeV, radial parameter $r_0 = r_C = 1.25$ fm and diffuseness $a = 0.65$ fm. This potential provides the $d-\alpha$ bound state with the binding energy $\varepsilon_{d\,\alpha} = 1.474$ MeV [58] . The corresponding bound-state wave number of the $d\,\alpha$ bound state is $\kappa_{d\,\alpha} = \sqrt{2\,\mu_{d\,\alpha}\,\varepsilon_{d\,\alpha}} = 0.31$ fm$^{-1}$. The square of ANC for the virtual decay ${}^6\mathrm{Li} \to d + \alpha$ is $[C_{(d\,\alpha)0}]^2 = 7.28$ fm$^{-1}$. This value is higher than a realistic value of this square of $[C_{(d\,\alpha)0}]^2 = 5.29$ fm$^{-1}$ [59]. To get the correct ANC from the one obtained in the Woods-Saxon potential we need to introduce the spectroscopic factor. However, because we are not interested in the absolute cross section, we keep using the ANC generated by the Woods-Saxon potential.

Usually the indirect experiments are performed at fixed incident energy of the projectiles [3]. In the case under consideration the projectile is ${}^6\mathrm{Li}$ or ${}^{12}\mathrm{C}$ (in the inverse kinematics). To cover the $E_{\alpha\,{}^{12}\mathrm{C}}$ energy interval $\sim 2$ MeV at fixed relative kinetic energy $E_{{}^6\mathrm{Li}\,{}^{12}\mathrm{C}}$, one needs to change $p_{d\,\alpha}$. Since $\mathbf{k}_{{}^6\mathrm{Li}}$ is fixed to change $p_{d\,\alpha}$ we have to change $\mathbf{k}_d$ so that $p_{d\,\alpha} \le \kappa_{d\,\alpha}$. It can be achieved by changing $k_d$ or its direction $\hat{\mathbf{k}}_d$ or both. Experimentally one can select all the events falling into the region $p_{d\,\alpha} \le \kappa_{\alpha\,d}$. Here, to simplify calculations, we assume that $\mathbf{k}_d || \mathbf{k}_{{}^6\mathrm{Li}}$. It means that the variation of $p_{d\,\alpha}$ is achieved by changing of $k_d$. Owing to the energy conservation by changing $k_d$ we can vary $E_{\alpha\,{}^{12}\mathrm{C}}$ but simultaneously we change the $d-\alpha$ relative momentum $p_{d\,\alpha}$. The triple differential cross section given by Eq. (45) is proportional to the $d-\alpha$ bound-state wave function in the momentum space $\varphi^2_{d\,\alpha}(p_{d\,\alpha})$, which decreases with increase of $p_{d\,\alpha}$, see Fig. 2.

To avoid significant decrease of the triple differential cross section when covering the $E_{\alpha\,{}^{12}\mathrm{C}}$ energy interval $\approx 2$ MeV it is better to take a lower $E_{{}^6\mathrm{Li}\,{}^{12}\mathrm{C}}$ but not too close to the Coulomb barrier in the initial channel of the indirect reaction (3). Taking into account that this Coulomb barrier is $\approx 5$ MeV we consider as an example the relative kinetic energy $E_{{}^6\mathrm{Li}\,{}^{12}\mathrm{C}} = 7$ MeV. In this case for $E_{\alpha\,{}^{12}\mathrm{C}} = 2.28$ MeV, which is close to the resonance energy of the $1^-$ resonance, $p_{d\,\alpha} = 0.141$ fm$^{-1}$ while at $E_{\alpha\,{}^{12}\mathrm{C}} = 0.3$ MeV $p_{d\,\alpha} = 0.281$ fm$^{-1}$. Hence, when covering the $E_{\alpha\,{}^{12}\mathrm{C}}$ energy interval from the energy $E_{\alpha\,{}^{12}\mathrm{C}} = 2.28$ MeV to the most effective astrophysical energy for the process ${}^{12}\mathrm{C}(\alpha,\,\gamma){}^{16}16$ the square of the Fourier transform $\varphi^2_{d\,\alpha}(p_{d\,\alpha})$ drops by a factor of 2.97. Note that the drop of $\varphi^2_{d\,\alpha}(p_{d\,\alpha})$, when moving from $E_{\alpha\,{}^{12}\mathrm{C}} = 2.28$ MeV to 0.9 MeV, is 2.1. $\varphi^2_{d\,\alpha}(p_{d\,\alpha})$ appears because we consider the indirect three-body reaction. There is another energy-dependent factor $\tilde{M}_L$, which is also result of the consideration of the three-body indirect reaction. This factor will be considered below.

Our goal is to calculate the photon's angular distributions at different $E_{\alpha-{}^{12}\mathrm{C}}$ energies. It can allow us to compare the indirect cross sections at higher energy $E_{\alpha-{}^{12}\mathrm{C}} = 2.28$ MeV and the most effective astrophysical energy $E_{\alpha-{}^{12}\mathrm{C}} = 0.3$ MeV. Because the indirect triple differential cross section does not contain the penetrability factor in the channel $\alpha-{}^{12}\mathrm{C}$ of the binary sub-reaction (2), the indirect method allows one to measure the triple differential cross section at $E_{\alpha-{}^{12}\mathrm{C}} = 0.3$ MeV what is impossible by any direct method.

1. By comparing the triple differential cross sections at higher energies and at 0.3 MeV we can determine how much the indirect cross section will drop when we reach $E_{\alpha-{}^{12}\mathrm{C}} = 0.3$ MeV. It will help to understand whether it is feasible to measure the triple differential cross section at such a low energy.
2. The second goal is to determine whether the interference of the $1^-$ subthreshold resonance and $1^-$ resonance at 2.423 MeV is constructive or distractive because the pattern of this interference may affect the photon's angular distribution.
3. The third goal is to compare the relative contribution of the $E1$ and $E2$ transitions.

TABLE I: Parameters used in calculations of the astrophysical factors of the $^{12}$C($\alpha$, $\gamma$)$^{16}$O radiative capture and the photon's angular distributions from the indirect $^{12}$C($^6$Li, $d\,\gamma$)$^{16}$O reaction.

| | $L=1$ | $L=2$ |
|---|---|---|
| $E_1$ [MeV] | ($-0.45$) | ($-0.245$) |
| $\gamma_{1\,0\,L\,L}$ [MeV$^{1/2}$] | (0.0867) | (0.1500) |
| $\gamma^L_{(\gamma)\,1\,0\,L\,L}$ [MeV$^{1/2}$fm$^{L+1/2}$] | (0.0241) | (0.9415) |
| $E_2$ [MeV] | 3.0 | 2.8 |
| $\gamma_{2\,0\,L\,L}$ [MeV$^{1/2}$] | 0.3254 | 0.75 |
| $\gamma^L_{(\gamma)\,2\,0\,L\,L}$ [MeV$^{1/2}$fm$^{L+1/2}$] | $-0.00963$ | $-0.09257$ |
| $E_3$ [MeV] | 33.8 | |
| $\gamma_{3\,0\,L\,L}$ [MeV$^{1/2}$] | 1.1 | |
| $\gamma^L_{(\gamma)\,3\,0\,L\,L}$ [MeV$^{1/2}$fm$^{L+1/2}$] | $-0.00239$ | |

### A. Astrophysical factors for $^{12}$C($\alpha$, $\gamma$)$^{16}$O

First, to determine the parameters, which we use to calculate the triple differential cross sections, we fit the experimental astrophysical factors $S_{E1}$ for the $E1$ transition and $S(E2)$ for the $E2$ transition for the $^{12}$C($\alpha$, $\gamma$)$^{16}$16 reaction from [19]. We do not pursue a perfect fit and are mostly interested in fitting energies below the $1^-$ resonance at 2.423 MeV, and at low energies $E_{\alpha-^{12}\mathrm{C}} \leq 1$ MeV. To get an acceptable fit for the $E1$ transition we needed to include three levels, two physical states, subthreshold $1^-$ state and the $1^-$ resonance, and one background state. For the $E2$ transition it was enough to include only two physical states, $2^+$ subthreshold resonance and $2^+$ resonance at 2.683 MeV.

We repeat that we do not pursue the perfect fit of the experimental $S$ factors. Our goal is to demonstrate the pattern of the triple differential cross section using reasonable parameters. More complicated fit can be done when indirect data will be available. In our fit, we kept fixed only the parameters of the subthreshold resonances $1^-$ and $2^+$ while the parameters of the higher lying resonances $1^-$ and $2^+$ were varying. The fixed parameters are shown in Table I in parentheses. In this table is shown the set of the parameters used to fit the astrophysical factors $S_{E1}$ and $S_{E2}$. These parameters are also used to calculate the triple differential cross section. $E_n$ is the energy of the $n$-th level.

Note that in the $R$-matrix approach, which includes a few interfering levels, it is convenient to choose one of the energy level coinciding with the location of the observable physical state [56, 60] while energies of other levels become fitting parameters.

In this paper we adopted $E_1 = -\varepsilon^{(s)}_{\alpha\,^{12}\mathrm{C}(1)} = -0.045$ MeV for $L=1$ and $E_2 = -\varepsilon^{(s)}_{\alpha\,^{12}\mathrm{C}(2)} = -0.245$ MeV for $L=2$ transitions. Then the boundary condition for the second and third levels of the $E1$ transition are taken at $E_{\alpha\,^{12}\mathrm{C}} = -0.045$ MeV while for $L=2$ the boundary condition is taken at $E_{\alpha\,^{12}\mathrm{C}} = -0.245$ MeV. Moreover, because in our choice the locations of the subthreshold bound states for $L=1$ and $L=2$ are fixed, the energies of other levels are fitting parameters and deviate from the real resonance energies. For example, the $1^-$ resonance at 2.423 MeV in the fit is shifted to $E_{\alpha\,^{12}\mathrm{C}} = 3.0$ MeV and the $2^+$ resonance at 2.683 MeV is shifted to 2.8 MeV. Hence, the statement that we take into account the radiative capture through the wing of the subthreshold $1^-$ resonance at $E_{\alpha\,^{12}\mathrm{C}} = -0.045$ MeV and the $1^-$ resonance at $E_{\alpha\,^{12}\mathrm{C}} = 2.423$ MeV does not contradict to the fact that in the fit the resonance at 2.423 MeV is shifted to 3.0 MeV. To fit the $E1$ transition we needed to add the background state at 33.8 MeV with parameters given in Table I.

In this table, the given parameters provide the constructive interference of the subthreshold $1^-$ resonance and resonance at 2.423 MeV at low energies. Changing the sign of $\gamma^1_{(\gamma)\,2\,0\,1\,L} = -0.00963$ MeV$^{1/2}$fm$^{3/2}$ to positive provides the destructive interference between the first two $1^-$ levels. In what follows by the $E1$ constructive (destructive) interference we mean the constructive (destructive) interference between the first two $1^-$ levels.

In Fig. 3 the calculated $S_{E1}$ and $S_{E2}$ astrophysical factors for the $E1$ and $E2$ transitions, respectively, are compared with the experimental ones from [19]. Our fitted astrophysical factors are: $S_{E1}(0.3\,\mathrm{MeV}) = 124.6$ keVb for the $E1$ transition and $S_{E2}(0.3\,\mathrm{MeV}) = 71.1$ keVb for the $E2$ transition. Evidently that our value for the $E1$ transition is higher than the contemporary accepted value of 80 keVb for constructive interference but the value for the $E2$ transition is close to the low value 60 keVb [37]. But, as we have underscored, our values should not be taken very seriously. In the absence of indirect data we use the parameters obtained from fitting the data from [19] to generate the photon's angular distributions to make some qualitative predictions. We also show how the photon's angular distributions are affected by lowering $S_{E1}(0.3\,\mathrm{MeV})$.

### B. Photon's angular distributions

In Figs. 4, 5, 6 and 7 the photon's angular distributions are shown at four different $E_{\alpha\,^{12}\mathrm{C}}$ energies: 0.3, 0.9, 2.1 and 2.28 MeV. We do not show the angular distributions at the middle energy 1.5 MeV because it is very similar to the angular distributions at higher energies and com-

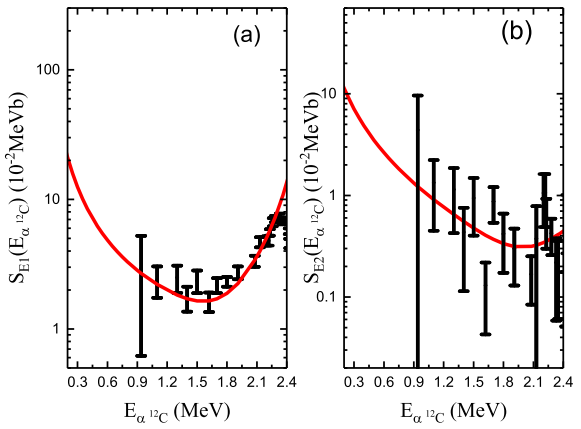


FIG. 3: Low-energy astrophysical $S_{E1}(E_{\alpha\,^{12}C})$ and $S_{E2}(E_{\alpha\,^{12}C})$ factors for $E1$ and $E2$ transitions for the $^{12}C(\alpha,\gamma)^{16}O$ radiative capture. Black dotes are astrophysical factors from [19], solid red line is present paper fit. Panel (a): $S_{E1}(E_{\alpha\,^{12}C})$ astrophysical factor; panel (b): $S_{E2}(E_{\alpha\,^{12}C})$ astrophysical factor.

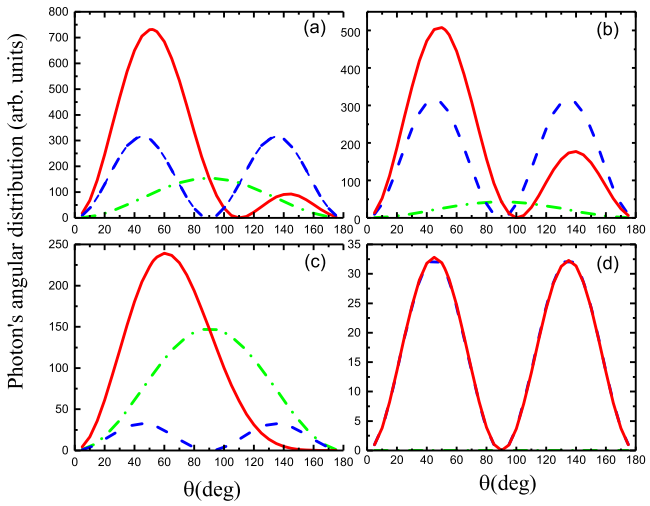


FIG. 4: Angular distribution of the photons emitted from the reaction $^{12}C(^6Li, d\gamma)^{16}O$ proceeding through the wings of two subthreshold resonances $1^-$, $E_{\alpha\,^{12}C} = -0.045$ MeV, $2^+$, $E_{\alpha\,^{12}C} = -0.245$ MeV, and the resonances at $E_{\alpha\,^{12}C} > 0$. The green dashed-dotted line is the angular distribution for the electric dipole transition $E1$, the blue dashed line is the angular distribution generated by the electric quadrupole $E2$ transition, and the red solid line is the total angular distribution resulted from the interference of the $E1$ and $E2$ radiative captures. Panel (a): $E_{\alpha\,^{12}C} = 0.3$ MeV, constructive interference of the $E1$ transitions through the wing of $1^-$, $E_{\alpha\,^{12}C} = -0.045$ MeV and the resonance $1^-, E_R = 2.423$ MeV; panel (b): $E_{\alpha\,^{12}C} = 0.3$ MeV, destructive interference of the $E1$ transitions through the wing of $1^-$, $E_{\alpha\,^{12}C} = -0.045$ MeV and the resonance $1^-, E_R = 2.423$ MeV; panel (c): the same as panel (a) for $E_{\alpha\,^{12}C} = 0.9$ MeV; panel (d): the same as panel (b) for $E_{\alpha\,^{12}C} = 0.9$ MeV.

pletely dominated by the $E1$ transition. The calculations are performed at $E_{^6Li\,^{12}C} = 7$ MeV (9.33 MeV in the Lab. system with $^6$Li projectile), which is higher than the Coulomb barrier $V_{CB} \approx 5$ MeV in the entry channel $^6Li + ^{12}C$ of the indirect reaction.

Figures 4 and 5 are very instructive. First, we note that the $E1$ angular distributions of the photons at all energies are peaked at 90° while the $E2$ angular distributions are double-humped and peaked at 45° and 135°. However, the interference of the $E1$ and $E2$ transitions leads to different total angular distributions. The angular distributions at 0.3 MeV are quite similar for the $E1$ transitions with constructive and destructive interferences, panels $(a)$ and $(b)$ in Fig. 4, with pronounced peaks at 52° and 50°, respectively. The character of the total angular distribution at 0.3 MeV depends on the relative weight of the $E1$ and $E2$ transitions.

The photon's angular distributions at 0.9 MeV, panels $(c)$ and $(d)$, are the most instructing. The patterns of the photon's angular distributions are different for the constructive and destructive $E1$ transitions what allows one to distinguish between two types of the $E1$ interferences. However, the cross sections for the destructive $E1$ interference is too small compared to the cross section at 0.3 MeV.

Now we proceed to the angular distributions at higher energies shown in Fig. 5. At higher energies, the $E1$ transition dominates and we see profound $E1$ type angular distributions both for the $E1$ constructive and destructive interferences of the two first $1^-$ levels. Hence, the angular distributions at higher energies cannot distinguish between constructive and destructive $E1$ interferences.

Comparing the relative values of the triple differential cross sections of Fig. 5, panel (c) and Fig. 4, panel (a) we can make, presumably, the most important conclusion: the triple differential cross section near the $1^-$ resonance at 2.28 MeV exceeds the one at 0.3 MeV by approximately an order of magnitude. We remind to the reader that in the case of the direct measurements when moving from 2.28 MeV to 0.3 MeV, the cross section drops by a factor of $10^9$. Our estimation detailed in the next section shows that measurements of the indirect triple differential cross section at 0.3 MeV are feasible. Thus, for the first time, we provide a possibility to measure the $^{12}C(\alpha,\gamma)^{16}O$ right at the most effective astrophysical energy 0.3 MeV.

In Figs 4 and 5 we have used the $R$-matrix parameters, which provide a higher $S_{E1}(0.3\,\mathrm{MeV}) = 124.6$ keVb for the constructive $E1$ transition than the contemporary accepted $\sim 80$ keVb [37]. To check how the photon's angular distributions are affected by a lower $E1$ astrophysical we changed three $R$-matrix parameters in Table I: $E_2 = 3.1$ MeV, $\gamma^1_{(\gamma)\,2\,0\,1\,1} = -0.006132$ MeV$^{1/2}$fm$^{3/2}$ and $\gamma_{3\,0\,1\,1} = 1.4$ MeV$^{1/2}$. With these parameters we get

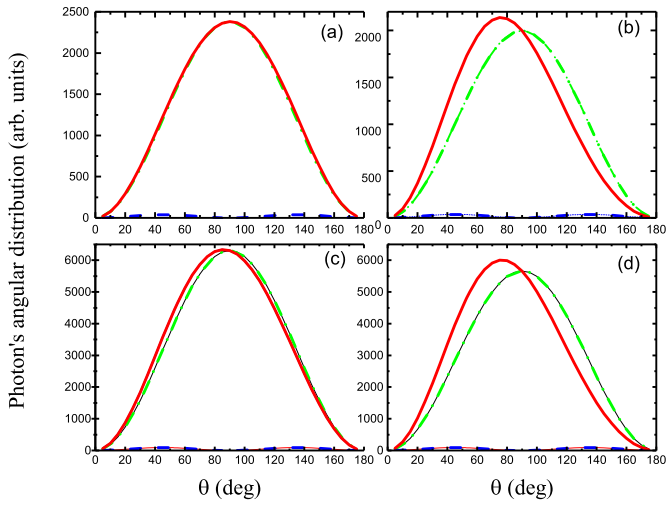


FIG. 5: Angular distribution of the photons emitted from the reaction $^{12}$C($^6$Li, $d\gamma$)$^{16}$O proceeding through the wings of the two subthreshold resonances, $1^-$, $E_{\alpha\,^{12}\mathrm{C}} = -0.045$ MeV, $2^+$, $E_{\alpha\,^{12}\mathrm{C}} = -0.245$ MeV, and the resonances at $E_{\alpha\,^{12}\mathrm{C}} > 0$. Notaions of the lines are the same as in Fig. 4. Panel (a): the same as panel (a) in Fig. 4 for $E_{\alpha\,^{12}\mathrm{C}} = 2.1$ MeV; panel (b): the same as panel (b) in Fog. 4 for $E_{\alpha\,^{12}\mathrm{C}} = 2.1$ MeV; panel (c) the same as panel (c) in Fig. 4 for $E_{\alpha\,^{12}\mathrm{C}} = 2.28$ MeV.

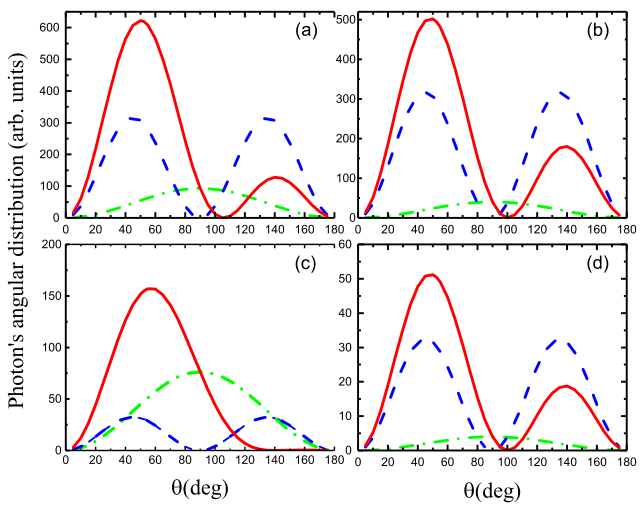


FIG. 6: The same as in Fig. 4 but the calculations are done with three modified $R$-matrix parameters generating lower $S_{E1}(0.3)$ MeV astrophysical factor.

$S_{E1}(0.3\,\mathrm{MeV}) = 75.8$ keVb and $S_{E1}(0.9\,\mathrm{MeV}) = 14.7$ keVb. We use the modified parameters to calculate the photon's angular distributions again at $E_{\alpha\,^{12}\mathrm{C}} =$ 0.3, 0.9, 2.1 and 2.28 MeV, see Figs 6 and 7. Thus we repeated calculations similar to the ones shown in Figs. 4 and 5 but with three modified parameters leading to smaller $S_{E1}$.

We find that decrease of the $S_{E1}$ does not change the angular distribution except for the panel (d) in 6, which is different than the panel (d) in Fig 4 but the absolute values of the cross sections in these panels are quite small. The main effect of the dropping of the $S_{E1}$ factor is a decrease of the triple differential cross section at higher energies where $E1$ significantly dominates over $E2$. As a result, the ratio of the triple differential cross sections at 2.28 MeV and 0.3 MeV is only 6.5. That is, the relative weight of the triple differential cross section at 0.3 MeV increases what makes more plausible the chances to measure the triple differential cross section at 0.3 MeV for lower $S_{E1}$.

In [37] it was underscored that contemporary experimental data do not exclude very low $S_{E1}(0.3\,\mathrm{MeV}) = 10$ keVb and high $S_{E2}(0.3\,\mathrm{MeV}) = 154$ keVb. We did not exploit here all the possibilities for the astrophysical factors but, evidently that this marginal values can change the photon's angular distributions. Indirect measurements can finally resolve ambiguities in the low-energy astrophysical factors.

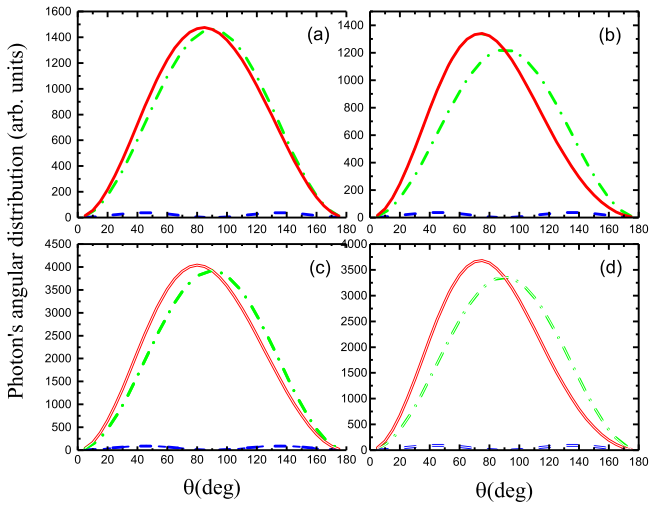


FIG. 7: The same as in Fig. 5 but calculations are done with three modified $R$-matrix parameters generating lower $S_{E1}(0.3)$ MeV astrophysical factor.

## V. FEASIBILITY OF THE PROPOSED APPROACH

Reliable estimates for the $^{12}$C($^6$Li,d) reaction cross section at 10-11 MeV energy of $^6$Li beam populating the $1^-$ state at 9.585 MeV can be made. Using FRESCO [61] reaction code and the same set of potentials as in [43], DWBA calculations predict cross section on the order of 10 mb/sr for forward angles (0-30° in c.m.). The $\gamma$

branching of this state to the $^{16}$O ground state is $5\times10^{-8}$ [58]. This sets the absolute scale for the cross sections to be measured at close to 1 nb. This is a very challenging but achievable target for a dedicated experimental setup. One possibility is to couple high efficiency array for high energy $\gamma$-rays (such as nearly $4\pi$ BaF or CsI [62–76] ) with large area position sensitive Si array (with total solid angle of $\sim 1$ sr) to detect deuterons. Another possibility is to use inverse kinematics ($^{12}$C beam on $^{6}$Li target) and detect $^{16}$O recoils in the spectrometer while still measuring deuterons at back angles in coincidence with high energy $\gamma$-rays. The former approach (direct kinematics) allows to achieve better energy resolution, while the later leads to very clean measurement due to triple $^{16}$O/$\gamma$/d coincidence. We estimate that event rates as high as $10^3$ per day can be achieved with high intensity beams (on the order of 1 particle $\mu$A) while keeping energy resolution within 100 keV. This specific estimate was made for the direct kinematics approach assuming 60 $\mu$g/cm$^2$ $^{12}$C target thickness. Slow variation of triple differential cross section with energy (by one order of magnitude) makes it possible to achieve satisfactory statistics even at $E_{\alpha\,^{12}\mathrm{C}} = 0.3$ MeV within reasonable time frame. One week of beam time would produce on the order of few hundred events in the region of Gamow window energy.

## VI. SUMMARY

In this paper, we suggested and developed the formalism of resonant indirect radiative capture reactions. The derived expressions for the triple and double differential cross sections can be used for the analysis of the indirect radiative capture reactions. The developed formalism can be utilized when indirect reactions proceed through a few subthreshold bound states and resonances. In this case, the statistical theory cannot be applied and the intermediate subthreshold bound states and resonances should be taken into account explicitly.

The idea of the indirect method is to use the indirect reaction $A(a, s\,\gamma)F$ to obtain the information about the radiative capture reaction $A(x,\,\gamma)F$, where $a = (s\,x)$ and $F = (x\,A)$. The main advantage of using the indirect reactions is the absence of the Coulomb-centrifugal penetrability factor in the entry channel $x + A$ of the binary sub-reaction $A(x,\,\gamma)F$, which suppresses the low-energy cross section of this reaction and does not allow one to measure it at astrophysically relevant energies.

Using indirect resonant radiative capture reactions one can obtain the information about important astrophysical resonant radiative capture reactions, like $(p,\,\gamma)$, $(\alpha,\,\gamma)$ and $(n,\,\gamma)$ on stable and unstable isotopes. The indirect technique makes accessible low-lying resonances, which are close to the threshold, and even subthreshold bound states at negative energies.

In this paper, after developing the general formalism, we have demonstated the application of the indirect method for the indirect reaction $^{12}$C($^{6}$Li$, d\,\gamma)^{16}$O proceeding through $1^-$ and $2^+$ subthreshold bound states and resonances to obtain the information about the $^{12}$C$(\alpha,\,\gamma)^{16}$O radiative capture.

The indirect method requires measurement of the triple differential cross section in the coincidence experiment, in which one has to measure the photon's angular distribution at given energy and scattering angle of the deuteron. This photon's angular distribution is the photon-deuteron angular correlation.

We show that the ratio of the triple differential cross section at energy $E_{\alpha\,^{12}\mathrm{C}} = 2.28$ MeV, which is close to the $1^-$ resonance at 2.423 MeV, to the one at $E_{\alpha\,^{12}\mathrm{C}} = 0.3$ MeV is about an order of magnitude. Such a small drop of the triple differential cross section when one reaches the most effective astrophysical energy $E_{\alpha\,^{12}\mathrm{C}} = 0.3$ MeV makes it possible to obtain the information about the astrophysical factor for the $^{12}$C$(\alpha,\,\gamma)^{16}$O process. We remind that in the direct experiment the cross section of the $^{12}$C$(\alpha,\,\gamma)^{16}$O reaction drops by $\sim 10^9$ when moving from the energies close to the resonance at 2.423 MeV down to 0.3 MeV. We discuss also the optimal experimental kinematics to measure the indirect reactions and, in particular, the $^{12}$C($^{6}$Li$,\,d\,\gamma)^{16}$O process.

## VII. ACKNOWLEDGMENTS

A.M.M. and G.V.R. acknowledge support from the U.S. DOE Grants No. DE-FG02-93ER40773. A.M.M. also acknowledges the support by the U.S. NSF Grant No. PHY-1415656. G.V.R. also acknowledges the financial support of the Welch Foundation (USA) (Grant No. A-1853). The authors thank the anonymous referee for the valuable comments which helped to improve the paper.

[1] H. A. Bethe, Phys. Rev. **55**, 103 (1939).
[2] C. E. Rolfs and W. S. Rodney, Cauldrons in the Cosmos, The University of Chicago Press, Chicago and London, 1988.
[3] R. E. Tribble, C. A. Bertulani, M. La Cognata, A. M. Mukhamedzhanov and C. Spitaleri, Rep. Prog. Phys. **77**, 106901 (2014).
[4] A. M. Mukhamedzhanov and N. K. Timofeyuk, JETP Lett. **51**, 282 (1990).
[5] A. M. Mukhamedzhanov, V. Kroha and M. La Cognata, Phys. Rev. **C 83** 044604 (2011).
[6] G. Baur, Phys. Lett. **B 178**, 135 (1986).
[7] C. Spitaleri *et al.*, Phys. Rev. **C 60**, 055802 (1999).
[8] A. M. Mukhamedzhanov, Phys. Rev. **C 84**, 044616 (2011).
[9] M. La Cognata *et al.* , Astrophys. J., **777**, 143 (2013).

[10] G. Baur *et al.*, Nucl. Phys. **A458**, 188 (1986 ).
[11] T. Motobayashi *et al.*, Phys. Rev. Lett. **73**, 2680 (1994).
[12] N. Austern, Direct nuclear reaction theories, Willey-Interscience, New-York, 1970.
[13] A. M. Mukhamedzhanov, Shubhchintal, and C. A. Bertulani, Phys. Rev. **C 96**, 024623 (2017).
[14] E. Burbidge, G. Burbidge, W. Fowler, and F. Hoyle, Rev. Mod. Phys. **29**, 547 (1957).
[15] W. Arnett, Annu. Rev. Astron. Astrophys. **11**, 73 (1973).
[16] C. Angulo *et al.*, Nucl. Phys. **A656**, 3 (1999).
[17] C. Abia *et al.*, Astrophys. J. **579**, 817 (2002).
[18] M. Lugaro *et al.*, Astrophys. J. **593**, 486 (2003).
[19] A. Redder *et al.*, Nucl. Phys. **A462**, 385 (1987).
[20] J. Ouellet *et al.*, Phys. Rev. C **54**, 1982 (1996).
[21] G. R. Caughlan and W. A. Fowler, At. Data Nucl. Data Tables **40**, 283 (1988).
[22] F. C. Barker, Aust. J. Phys. **31**, 27 (1978).
[23] F. C. Barker, Austr. J. Phys. **40**, 25 (1987).
[24] F. C. Barker and T. Kajino, Austr. J. Phys., **44**, 369 (1991).
[25] R.E. Azuma *et al.*, Phys. Rev. **C 50**, 1194 (1994).
[26] R. Azuma *et al.*, Phys. Rev. **C 56**, 1655 (1997).
[27] C. R. Brune, W. H. Geist, W. H. Kavanagh and K. D. Veal, Phys. Rev. Lett. **83**, 4025 (1999).
[28] C. Brune *et al.*, Nucl. Phys. **A688**, 263c (2001).
[29] R. Kunz, M. Jaeger, A. Mayer, J. W. Hammer, G. Staudt, S. Harissopulos, and T. Paradellis, Phys. Rev. Lett. **86**, 3244 (2001).
[30] J. W. Hammer *et al.*, Nucl.Phys. **A752**, 514c (2005).
[31] J. W.Hammer *et al.*, Nucl. Phys. **758**, 363c (2005).
[32] M. Assunção *et al.*, Phys. Rev. **C 73**, 055801 (2006).
[33] R. Plag *et al.*, Phys. Rev. **C 86**, 015805 (2012).
[34] D. Schürmann *et al.*, Eur. Phys. J. **A 26**, 301 (2005).
[35] D. Schürmann *et al.*, Eur. Phys. J. **A 26**, 301 (2006).
[36] D. Schürmann, L. Gialanella, R. Kunz, F. Strieder; Phys. Lett. **B711**, 35 (2012).
[37] Moshe Gai, arXiv: 1506.04501 [nucl-ex] (2015).
[38] D. B. Sayre, C. R. Brune, D. E. Carter, D. K. Jacobs, T. N. Massey, and J. E. ODonnell, Phys. Rev. Lett. **109**, 142501 (2012).
[39] M. Gai, Phys. Rev. **C 88**, 062801(R) (2013).
[40] C. R. Brune and D. B. Sayre, J. Phys.: Conference Series **420**, 012140 (2013).
[41] M. Gai, Nucl. Phys. **A928**, 313 (2014).
[42] M. Gai *et al.*, J. Instrum. **5**, 12004 (2010).
[43] M. L. Avila, G. V. Rogachev, E. Koshchiy, *et al.*, Phys. Rev. Lett. **114**, 071101 (2015).
[44] R. J. Jaszczak, J. H. Gibbons, and R. L. Macklin, Phys. Rev. **C 2**, 63 and 2452 (1970).
[45] P. Dyer and C. A. Barnes, Nucl. Phys. **A233**, 495 (1974).
[46] K. U. Kettner *et al.*, Z. Phys. **A308**, 73 (1982).
[47] M.W. Ahmed *et al.*, arXiv: 1307.8178 (2013).
[48] C. Vaccarezza *et al.*, Proceedings of IPAC2012, New Orleans, Louisiana, USA (2012).
[49] P. Tischhauser *et al.*, Phys. Rev. **C 79**, 055803 (2009).
[50] C. A. Bertulani and T. Kajino, Prog. Part. Nucl. Phys. **89**, 56 (2016).
[51] A. M. Mukhamedzhanov and R. E. Tribble, Phys. Rev. **C 59**, 3418 (1999).
[52] M. La Cognata1 *et al.*, Astrophys. J. **708**, 796 (2010)
[53] M. L. Sergi *et al.*, Phys. Rev. **C 82**, 032801(R) (2010).
[54] M. Gulino *et al.*, Phys. Rev. **C 87**, 012801(R) (2013).
[55] A. M. Lane and R. G. Thomas, Rev. Mod. Phys. **30**, 257 (1958).
[56] A. M. Mukhamedzhanov, Shubhchintak, C. A. Bertulani, Phys. Rev. **C 93**, 045805 (2016).
[57] A. M. Mukhamedzhanov, Shubhchintak, C. A. Bertulani, and T. V. Nhan Hao, Phys. Rev. **C 95**, 024616 (2017).
[58] D.R. Tilley *et al.*, Nucl. Phys. **A595**, 1 (1995).
[59] L. D. Blokhintsev, V. I. Kukulin, A. A. Sakharuk, D. A. Savin, E. V. Kuznetsova, Phys. Rev. **C 48**, 2390 (1993).
[60] F. C. Barker, Phys. Rev. **C 78**, 044611 (2008).
[61] I.J. Thompson, Comput. Phys. Rep. **7**, 167 (1988).
[62] M. Laval, Nuclear Instruments and Methods in Physics Research Section A: Accelerators, Spectrometers, Detectors and Associated Equipment **206**, 169 (1983).
[63] E. Dafni, Nuclear Instruments and Methods in Physics Research Section A: Accelerators, Spectrometers, Detectors and Associated Equipment, **254**, 54 (1987).
[64] T. Murakami *et al.*, Nuclear Instruments and Methods in Physics Research Section A: Accelerators, Spectrometers, Detectors and Associated Equipment, **253**, 163 (1986).
[65] R.A. Kryger *et al.*, Nuclear Instruments and Methods in Physics Research Section A: Accelerators, Spectrometers, Detectors and Associated Equipment, **346** 544 (1994).
[66] Takeshi Seo, Nuclear Instruments and Methods in Physics Research Section A: Accelerators, Spectrometers, Detectors and Associated Equipment, **325**, 176 (1993).
[67] R. Nicolini *et.al*, Nuclear Instruments and Methods in Physics Research Section A: Accelerators, Spectrometers, Detectors and Associated Equipment, **582**, 554 (2007).
[68] K. Wisshak **et al.**, Nuclear Instruments and Methods in Physics Research Section A: Accelerators, Spectrometers, Detectors and Associated Equipment, **A 292**, 595 (1990).
[69] J. L. Dugan **et al.**, International conference on the application of accelerators in research and industry, Denton, TX (United States), 201 (1994).
[70] M.Y. Lee **et al.**,Nuclear Instruments and Methods in Physics Research Section A: Accelerators, Spectrometers, Detectors and Associated Equipment, **A 422**, 536 (1999).
[71] S. K Rathi **et al.**, Nuclear Instruments and Methods in Physics Research Section A: Accelerators, Spectrometers, Detectors and Associated Equipment **482**, 355 (2002).
[72] H. Mach **et al.**, Proceedings of the Eleventh International Symposium, Pruhonice, Prague, Czech Republic,476 (2002).
[73] F. D. Becchetti **et al.**, Nuclear Instruments and Methods in Physics Research Section A: Accelerators, Spectrometers, Detectors and Associated Equipment, **A505**, 377 (2003).
[74] S. Cross **et al.**, Journal of Instrumentation,**6**, P08008 (2011).
[75] G. Mukherjee **et al.**, Proceedings of the DAE-BRNS symposium on nuclear physics, Mumbai (India) 57, 872 (2012).
[76] E. Migneco *et al.*, Nuclear Instruments and Methods in Physics Research Section A: Accelerators, Spectrometers, Detectors and Associated Equipment, **314**, 31 (1992).